Journal of the American Heart Association

ORIGINAL RESEARCH

Flow-Induced Secretion of Endothelial Heparanase Regulates Cardiac Lipoprotein Lipase and Changes Following Diabetes

Chae Syng Lee, MSc; Yajie Zhai, MSc; Rui Shang, BSc; Trevor Wong; Aurora J. Mattison, BSc; Haoning Howard Cen, PhD; James D. Johnson, PhD; Israel Vlodavsky, PhD; Bahira Hussein, MSc; Brian Rodrigues, PhD

BACKGROUND: Lipoprotein lipase (LPL)-derived fatty acid is a major source of energy for cardiac contraction. Synthesized in cardiomyocytes, LPL requires translocation to the vascular lumen for hydrolysis of lipoprotein triglyceride, an action mediated by endothelial cell (EC) release of heparanase. We determined whether flow-mediated biophysical forces can cause ECs to secrete heparanase and thus regulate cardiac metabolism.

METHODS AND RESULTS: Isolated hearts were retrogradely perfused. Confluent rat aortic ECs were exposed to laminar flow using an orbital shaker. Cathepsin L activity was determined using gelatin-zymography. Diabetes was induced in rats with streptozotocin. Despite the abundance of enzymatically active heparanase in the heart, it was the enzymatically inactive, latent heparanase that was exceptionally responsive to flow-induced release. EC exposed to orbital rotation exhibited a similar pattern of heparanase secretion, an effect that was reproduced by activation of the mechanosensor, Piezo1. The laminar flow-mediated release of heparanase from EC required activation of both the purinergic receptor and protein kinase D, a kinase that assists in vesicular transport of proteins. Heparanase influenced cardiac metabolism by increasing cardiomyocyte LPL displacement along with subsequent replenishment. The flow-induced heparanase secretion was augmented following diabetes and could explain the increased heparin-releasable pool of LPL at the coronary lumen in these diabetic hearts.

CONCLUSIONS: ECs sense fluid shear-stress and communicate this information to subjacent cardiomyocytes with the help of heparanase. This flow-induced mechanosensing and its dynamic control of cardiac metabolism to generate ATP, using LPL-derived fatty acid, is exquisitely adapted to respond to disease conditions, like diabetes.

Key Words: cardiomyocytes ■ endothelial cells ■ heparanase ■ lipoprotein lipase ■ mechanosensors

The heart has a high demand for energy because of its continuous and rhythmic pumping. Accordingly, it uses multiple sources of chemical energy to generate ATP for mechanical contraction, including fatty acids (FA), glucose, lactate, ketones, and amino acids.[1] In fact, in the human heart, FAs were recently reported to be the primary substrate consumed.[2] As the heart cannot synthesize FA, it relies on obtaining it from other sources. These include adipose tissue, breakdown of endogenous cardiac triglyceride, and lipolysis of circulating triglyceride-rich lipoproteins by lipoprotein lipase (LPL) located at the endothelial cell (EC) surface of the coronary lumen.[3,4] LPL-derived FA is considered a major source of energy for cardiac contraction.[2]

In the heart, LPL is produced in cardiomyocytes and subsequently secreted onto heparan sulphate proteoglycan (HSPG) binding sites on the cardiomyocyte apical surface.[5,6] HSPG consists of a core protein to which several linear heparan sulphate (HS) side chains

Correspondence to: Brian Rodrigues, Faculty of Pharmaceutical Sciences, UBC, 2405 Wesbrook Mall, Vancouver, BC, Canada V6T 1Z3.
Email: rodrigue@mail.ubc.ca

Supplemental Material is available at https://www.ahajournals.org/doi/suppl/10.1161/JAHA.122.027958

For Sources of Funding and Disclosures, see page 15.

JAHA is available at: www.ahajournals.org/journal/jaha

CLINICAL PERSPECTIVE

What Is New?

- This study reports on the ability of endothelial cells to sense fluid shear stress and communicate this information to subjacent cardiomyocytes with the help of heparanase.
- Unlike the conventional link between mechanosensors and management of vascular tone, this study describes a novel role of endothelial mechanosensors in regulation of cardiac metabolism, especially fatty acid delivery to the heart.

What Are the Clinical Implications?

- Understanding flow-induced mechanosensing and its dynamic control of cardiac metabolism to generate ATP using lipoprotein lipase-derived fatty acids may offer insights into potential mechanism-driven therapeutic interventions in a metabolic disease, like diabetes.

Nonstandard Abbreviations and Acronyms

EC	endothelial cell
Hpa^{A}	active heparanase
Hpa^{L}	latent heparanase
HSPG	heparan sulfate proteoglycan
LF	laminar flow
LPL	lipoprotein lipase
P^{Fr}	perfusate fractions

are linked and function not only as structural proteins but also as anchors because of the high content of charged groups in HS.[7] The latter property is used to electrostatically bind a bioactive protein like LPL, providing the cell with a rapidly accessible reservoir, thus precluding the need for de novo synthesis when there is immediate requirement for this enzyme.[5,6] Thus, the cardiomyocyte demand for FAs to drive ATP synthesis can be resolved, not by synthesizing more LPL, but simply translocating enzyme from this surface pool to the vascular lumen. For this to materialize, LPL requires shedding from HSPG and navigation across the interstitial space.[8] GPIHBP1 (GPI-anchored high-density lipoprotein-binding protein 1) at the basolateral side of EC then transports LPL to the apical side (surface facing the coronary lumen).[8,9] Out here, GPIHBP1 also functions as a platform to enable vascular LPL to hydrolyze lipoprotein-triglyceride to FA.[10,11]

Detachment of LPL from the cardiomyocyte surface is mediated by cleavage of HSPG by heparanase.[12,13] Heparanase is an endoglycosidase, exceptional in its ability to degrade HS.[14] It is synthesized in the EC as an enzymatically inactive, latent heparanase (Hpa^{L}) 65-kDa enzyme that undergoes cellular secretion followed by HSPG-facilitated reuptake.[15,16] After proteolytic cleavage in lysosomes, a 50-kDa highly active polypeptide is formed (active heparinase [Hpa^{A}]).[17,18] Lysosomes store Hpa^{A} until mobilized to act on subjacent cardiomyocyte HS to release LPL. Intriguingly, Hpa^{L} also has some remarkable properties, including its ability to activate signaling elements[13,16,19–21] and capacity to be taken up by adjacent cells that do not express heparanase, where it can modulate gene expression.[22]

Lining the inner layer of coronary vessels, ECs are continuously subjected to blood flow-mediated biophysical forces, including laminar flow (LF). By sensing this mechanical force, EC mechanosensors convert LF into a biochemical signal (eg, release of nitric oxide)[23] to maintain vascular tone.[24] Whether LF can also contribute toward the regulation of cardiac metabolism is largely undetermined. We hypothesized that LF can also cause ECs to secrete heparanase. In this way, in addition to its established role in dilation or constriction of blood vessels, the EC may act as a decision-making cell in cardiac metabolism, given the unique responsibility of heparanase to release myocyte LPL for forward movement to the vascular lumen. Our data suggest that the EC response to LF is a key instigator for heparanase release, a process that is enhanced following diabetes to meet the altered energy demands of the heart.

METHODS

The data, methods used in the analysis, and materials used to conduct the research will be available to any researcher for purposes of reproducing the results or replicating the procedure upon request to the corresponding author.

Experimental Animals

This investigation conforms to the *Guide for the Care and Use of Laboratory Animals* published by the National Institutes of Health, the Canadian Council on Animal Care Guidelines, and institutional guidelines at University of British Columbia (Certificate A17-0072). Rats were euthanized using a single dose of 100 mg/kg intraperitoneal injection of sodium pentobarbital (Euthanyl). Once toe pinch and corneal reflexes were lost, a thoracotomy was performed before removal of the heart. Male Wistar rats (Charles River Laboratories, Canada) between 7 to 9 weeks were obtained and hearts from these animals used for Langendorff retrograde perfusion and isolation of ventricular cardiomyocytes. Where indicated, diabetes was induced in these rats by intravenous injection of streptozotocin (55 mg/kg; diabetes). For this procedure, rats were transiently anesthetized with isoflurane (University of British

Columbia; Animal Care Committee-01-2017) using an isoflurane vaporizer. The flow rate of isoflurane exposure was slowly increased to 5% over ≈5 minutes. Rats were removed from the induction chamber, a nose cone applied, and the isoflurane vaporizer adjusted to 2%. Once the animal did not respond to toe pinch, streptozotocin was injected into the tail vein. After 24 hours, hyperglycemia (>13 mmol/L) was confirmed in tail-tip blood samples using a glucometer and glucose test strips. Diabetic animals were followed for 4 days before termination, at which point blood in the thoracic cavity was collected in K2-EDTA tubes and centrifuged immediately for separation of plasma that was used for determination of insulin (rat insulin ELISA; ALPCO).

Langendorff Heart Perfusion

Following anesthesia, the thoracic cavity was exposed and hearts were quickly removed. Subsequently, hearts were placed in ice-cold Krebs-Ringer HEPES buffer, and the aorta was canulated. Hearts were then retrogradely perfused in the nonrecirculating mode where the rate of coronary flow was maintained between 7 and 8 mL/min using a pump (Masterflex). Perfusion buffer was gassed with 95% O_2 and 5% CO_2 in a double-walled water-heated chamber where the temperature was controlled using a circulating water bath and kept at 37 °C. Once the blood was washed from the coronary blood vessels and a clear perfusate was visible, the coronary effluent was collected over a period of 30 minutes. The samples over 5-minute intervals were pooled and concentrated, using an Amicon 30K filtration unit, to 40 μL. These concentrated perfusate fractions (P^{Fr}) were either analyzed for heparanase using Western blot or used as a source of EC-secreted heparanase to treat cardiomyocytes (only the initial 5-minute fraction).

Preparation of Cardiac Myocytes

Calcium-tolerant cardiomyocytes were prepared using a previously described procedure.[25] Briefly, following aortic cannulation, the heart was perfused retrogradely with collagenase (0.1%). The isolated cells were made calcium-tolerant by sequential exposure to increasing calcium concentrations. This method produces cells that are rod-shaped with clear cross-striations, yielding high viability (>70%). Cardiomyocytes were plated on 2% laminin-coated culture dishes in Medium 199 and allowed to settle for 2 hours. The medium was changed to remove unattached cells. Fresh medium was used before any experiments.

Release of LPL and Measurement of Its Activity

To evaluate the effect of heparanase on cell surface LPL, cardiomyocytes were incubated with either recombinant heparanase or P^{Fr} for 30 minutes. After this time, LPL activity was determined in the incubation medium. The results were compared with myocytes treated with heparin (2 U/mL). To measure LPL replenishment after its release from cardiomyocytes, cells were initially treated with heparin (2 U/mL) for 5 minutes to remove HSPG-bound LPL. Following washes to eliminate any residual heparin, myocytes were then incubated with recombinant heparanase and P^{Fr} at 37 °C for 2 hours, to allow the refilling of the cardiomyocyte HSPG with LPL. After this, the incubation medium was removed and replaced with fresh buffer containing heparin (2 U/mL) to determine the recovery of LPL at the cell surface. In some experiments, heparin was also used to quantify the amount of LPL at the coronary lumen of controls and diabetic hearts. In this case, isolated hearts were retrogradely perfused with 5 U/mL heparin, and the effluents were collected every 15 seconds over 5 minutes. LPL activity in the myocyte medium or the coronary perfusates was measured by in vitro hydrolysis of sonicated [^{3}H] triolein substrate emulsion as previously reported.[25]

EC Culture and Shear Stress Model

Rat aortic endothelial cells were cultured at 37 °C in a 5% CO_2 humidified incubator. Cells under passage 5 to 9 (from 3 different starting batches) were used at confluency for the experiments. To expose cells to LF, we used a system described by dela Paz et al.[26] Briefly, a 100-mm culture plate was modified by attaching a 60-mm culture plate to its center using medical adhesive. ECs were seeded onto the periphery of the larger plate and grown until confluence (about 7 days). Confluent ECs were exposed to LF using an orbital shaker inside a humidified incubator (5% CO_2 at 37 °C) for 30 minutes. The rotational speed was maintained at 250 rpm, yielding ≈15 dynes/cm^2 (physiological arterial shear stress is generally between 6 and 40 dynes/cm^2).[26] EC on an identical modified plate was kept as a static control. After 30 minutes of LF, the medium and cell lysates were collected separately. The medium was concentrated using an Amicon 30K filtration unit. Both medium and cell lysates were used for measurement of heparanase and other intracellular signaling molecules, using Western blot.

Cell Transfection of Small Interfering RNA

Small interfering (si)RNA for Piezo1 was purchased from Life Technologies (Silencer Select siRNA; s167339; sense: CAAGAAGUACAAUCAUCUAtt, antisense: UAGAUGAUUGUACUUCUUGgt). Silencer Select Negative Control No.1 siRNA (#4390843) was used as a negative control. ECs were grown in either 6-well plates or modified 100-mm plates and siRNA transfection was performed at 60% to 80% confluency.

Lipofectamine RNAiMAX (Life Technologies; #13778) was used for siRNA transfection according to the manufacturer's protocol. Cells were analyzed 48 hours after transfection. For heparanase secretion analysis, transfected cells in modified 100-mm plates were washed with PBS and fresh media applied before exposure to LF using orbital shaker.

Western Blot Analysis

Cell lysates were collected from either ECs and cardiomyocytes and analyzed using Western blot. Cells were washed with PBS, followed by lysis in ice-cold lysis buffer (1% Triton X-100, 0.1% SDS, 1 mmol/L phenylmethylsulfonyl fluoride, 1 mmol/L Na_3VO_4, 1× Protease inhibitor cocktail, 1× Phosphatase inhibitor, 5 mmol/L EDTA and 1 mmol/L ethylene glycol-bis(β-aminoethyl ether)-N,N,N′,N′-tetraacetic acid). The collected lysates were sonicated and centrifuged at 16,000*g* for 15 minutes at 4 °C. The supernatant obtained was used for determination of protein content using a Bradford assay kit (Bio-Rad). Equal amounts of proteins were separated by 10% SDS-PAGE, followed by transfer onto nitrocellulose membranes. Subsequently, membranes were either blocked with 5% (w/v) milk in Tris-buffered saline Tween-20 or Licor blocking buffer for 1 hour. The membranes were subsequently incubated with primary antibodies overnight at 4 °C. This was followed by Tris-buffered saline Tween-20 washes and the blots incubated with corresponding secondary IRDye antibodies for 1 hour at room temperature. Membranes were visualized and bands quantified using Li-Cor Odyssey CLX imaging system.

Cathepsin L Zymography

Protein concentration was determined using a Bradford assay, and samples were prepared to 0.5 to 1 μg/μL using 5× nonreducing sample denaturing buffer as previously described.[27] Samples were resolved in 12.5% polyacrylamide gels with 0.2% gelatin. Following sample run, gels were washed with 50 mmol/L Tris–hydrochloric acid renaturing buffer (pH 7.4). Subsequently, gels were incubated with activity buffer containing 0.1 mol/L sodium acetate–acetic acid, 2 mmol/L dithiothreitol, 1 mmol/L EDTA, pH 5.5 at room temperature for 30 minutes with shaking. The buffer was decanted and fresh activity buffer added and incubated overnight at 37 °C. Gels were washed with Milli-QH_2O and stained for 1 hour with Coomassie blue staining solution, 10% (v/v) acetic acid, 25% (v/v) isopropanol, and 0.045% (w/v) Coomassie brilliant blue R-250. Gels were incubated for 1 hour with destaining solution, 10% (v/v) acetic acid and 10% (v/v) isopropanol. To validate the molecular weight, 50 ng of recombinant cathepsin L (CatL; Sigma) was used in a 400 mmol/L sodium acetate pH 5.5, 4 mmol/L EDTA, 8 mmol/L dithiothreitol buffer. CatL activity is indicated by gel digestion. Bands were visualized by white light scanning at 600 dpi and quantified with ImageJ (version 1.5.1).

Intracellular Calcium

For the measurement of intracellular calcium concentration ($[Ca^{2+}]_i$), ECs grown on glass coverslips were loaded with a Ca^{2+} fluorescent dye Fura-2 acetoxymethyl ester (Fura-2-AM) in culture medium for 30 minutes. Following a 30-minute wash with Ringer buffer, the coverslips were mounted on a Zeiss Axiovert 200 mol/L inverted microscope (Carl Zeiss). A fresh buffer containing 1 μmol/L Yoda1 (an agonist for the mechanosensor Piezo1) was added after measuring the basal intracellular Ca^{2+} levels. Fura-2 was excited at 340 and 380 nm, and results were expressed as the ratio of the fluorescence emission intensity (F_{340}/F_{380}).

Quantitative Real-Time Polymerase Chain Reaction

Total RNA was isolated from ECs and cardiomyocytes using TRIzol (Invitrogen). RNA was reverse transcribed into cDNA using a mixture of dNTPs, oligo-(dT_{12-18}), and SuperScript II Reverse Transcriptase. cDNA was amplified by TaqMan probes (β-actin, heparanase, vascular endothelial growth factor A) in triplicate, using StepOnePlus Real-Time PCR system (Applied Biosystems). Gene expression was calculated by the comparative cycle threshold (ΔΔCT) method.

Statistical Analysis

Prism 9 (version 9.3.0) GraphPad Software (San Diego, California, USA) was used to statistically analyze the data. The Shapiro–Wilk test was performed to determine the normality of the data. The Student *t*-test were used to determine 2 group mean values. When appropriate, 1-way ANOVA was used followed by Bonferroni post hoc comparison test. Data are expressed in mean±SEM. Minimal statistical significance was set at $^*P<0.05$.

Materials

Rat aortic endothelial cells were obtained from Cell Applications. Streptozotocin and other chemicals were obtained from Sigma. Heparin was from Sandoz (10 000 U/mL). Purified Hpa^L was prepared as described,[28] and Hpa^A was purchased from R&D (#7570-GH). Yoda1 and 2-methylthioadenosine 5′-triphosphate (2-MeSATP) were purchased from Tocris Bioscience (#5586 and #1062). The G-actin/F-actin In Vivo Assay Biochem Kit was obtained from Cytoskeleton Inc. (Denver, CO). ATP Determination Kit was obtained from Invitrogen (#A22066). [^{3}H]-triolein was purchased from Perkin-Elmer (NET431001MC). Anti-heparanase

antibody HP3/17 was from Prospec (Rehovot, Israel), which recognizes both the active (50-kDa) and latent (65-kDa) form of heparanase. All other antibodies were obtained from Cell Signaling Technology, Santa Cruz Biotechnology, and Millipore, including phospho-protein kinase D (pPKD; #2054), total protein kinase D (PKD; #SC-935), phospho-P38-mitogen activated protein kinase (pP38MAPK; #9211), total P38-mitogen activated protein kinase (P38MAPK; #9212), vinculin (#13901), and α-tubulin (#05–829).

RESULTS

Retrograde Langendorff Heart Perfusion Releases Heparanase Into the Coronary Effluent

To identify and measure heparanase protein expression in cardiac tissue, whole hearts were isolated and blotted for Hpa^L and Hpa^A. Compared with Hpa^L, Hpa^A was the dominant form present, exhibiting an almost 40-fold higher amount (Figure 1A). We used the Langendorff heart to determine whether cardiac Hpa can be released into the perfusate by fluid under constant pressure and flow (Figure 1B, *left panel*). Despite the abundance of tissue Hpa^A, it was the Hpa^L that was exceptionally responsive to flow-induced release. As such, within the first 5 minutes of perfusion initiation, the highest amount of Hpa^L was detected in the concentrated coronary perfusates, with a gradual decline in secretion over the next 30 minutes (Figure S1; Figure 1B, *right panel*). For Hpa^A, the initial and overall amount released was substantially lower, with a complete cessation of secretion at 30 minutes, suggesting that of the large storage pool of Hpa^A, only a small fraction of this pool is responsive to flow-mediated release (Figure 1B, *right panel*). Other secreted proteins from EC, such as von Willebrand factor, were not identified in the whole heart perfusates (*data not shown*). To determine residual tissue heparanase following perfusion for 30 minutes, hearts were blotted for both forms and the results compared with nonperfused hearts. The robust release of Hpa^L resulted in an almost complete absence of its residual amount in the heart following perfusion (Figure 1C). Conversely, with minimal flow-induced release of Hpa^A into the coronary perfusate, the cardiac pool of Hpa^A remained largely unchanged despite sustained perfusion for 30 minutes. Our data suggest that of the 2 forms of heparanase, Hpa^L is the one that is more responsive to coronary flow-induced release.

Laminar Flow Stimulates Heparanase Secretion From ECs

In the heart, ECs outnumber cardiomyocytes.[29] Intriguingly, it is the EC that is the predominant cell type to express heparanase, with negligible amount of *Hpa1* gene expression in cardiomyocytes[30] (Figure S2). To determine if the pattern of heparanase protein expression in the whole heart (Figure 1A) can be explained by the content in ECs, we used ECs to analyze Hpa^L and Hpa^A. As anticipated, this cell type exhibited a more robust expression of Hpa^A over Hpa^L (Figure 2A). Using a modified 100-mm culture dish, we validated our orbital flow model of laminar shear stress (Figure 2B). Indeed, as reported previously, gene expression of *Vegfa* following 3 days of orbital rotation[26] (Figure S3A), or phosphorylation of AKT at S473 after 30 minutes[31] were augmented (Figure S3B). Next, we evaluated whether EC release heparanase in response to LF. Intriguingly, when compared with ECs under static conditions, LF rapidly released both Hpa^L and Hpa^A. This response was time-dependent (Figure 2C) and exhibited a similar pattern as observed in the Langendorff perfused heart, a more robust release of Hpa^L over Hpa^A (Figure 2C, *inset*). We tested whether the effect of LF on EC heparanase release is through mechanosensors, like Piezo1, using a selective Piezo1 agonist Yoda1. ECs use mechanosensors that are widely known to sense the mechanical force generated by LF, converting it into a biochemical signal[23] that maintains vascular tone.[24] Confirmation of Piezo1 activation was done by measuring Ca^{2+} influx, which was augmented after Yoda1 (Figure 2D). Strikingly, Yoda1 demonstrated significant Hpa^L secretion (Figure 2E), an effect that was inhibited following Piezo1 knockdown using siRNA (Figure S4) or a selective antagonist of Piezo1 (Figure S5). It should be noted that testing of another mechanosensor like focal adhesion kinase using an activator like Zinc40099027[32] was unable to release heparanase (*data not shown*). These results validate our hypothesis that LF-induced mechanosignaling mediates heparanase release.

Purinergic Receptor Activation Is Required for Laminar Flow-Mediated Release of Heparanase from ECs

Previously, we observed that ECs are capable of releasing both Hpa^L and Hpa^A in response to high glucose (HG), an effect mediated by release of ATP followed by purinergic receptor activation.[33] In the present study, we compared the secretion of heparanase and ATP by HG to that by LF. The osmolality control, mannitol, had no effect on medium heparanase secretion (Figure S6). LF was a superior stimulus to release Hpa^L (Figure 3A) and could be linked to the earlier release of ATP compared with HG (Figure 3B). We used 2-MeSATP, an ATP analog that can act as an ATP-activated purinergic receptor (P2Y) agonist, to validate the contribution of ATP to EC heparanase secretion. Within 30 minutes, 2-MeSATP triggered a robust secretion of both

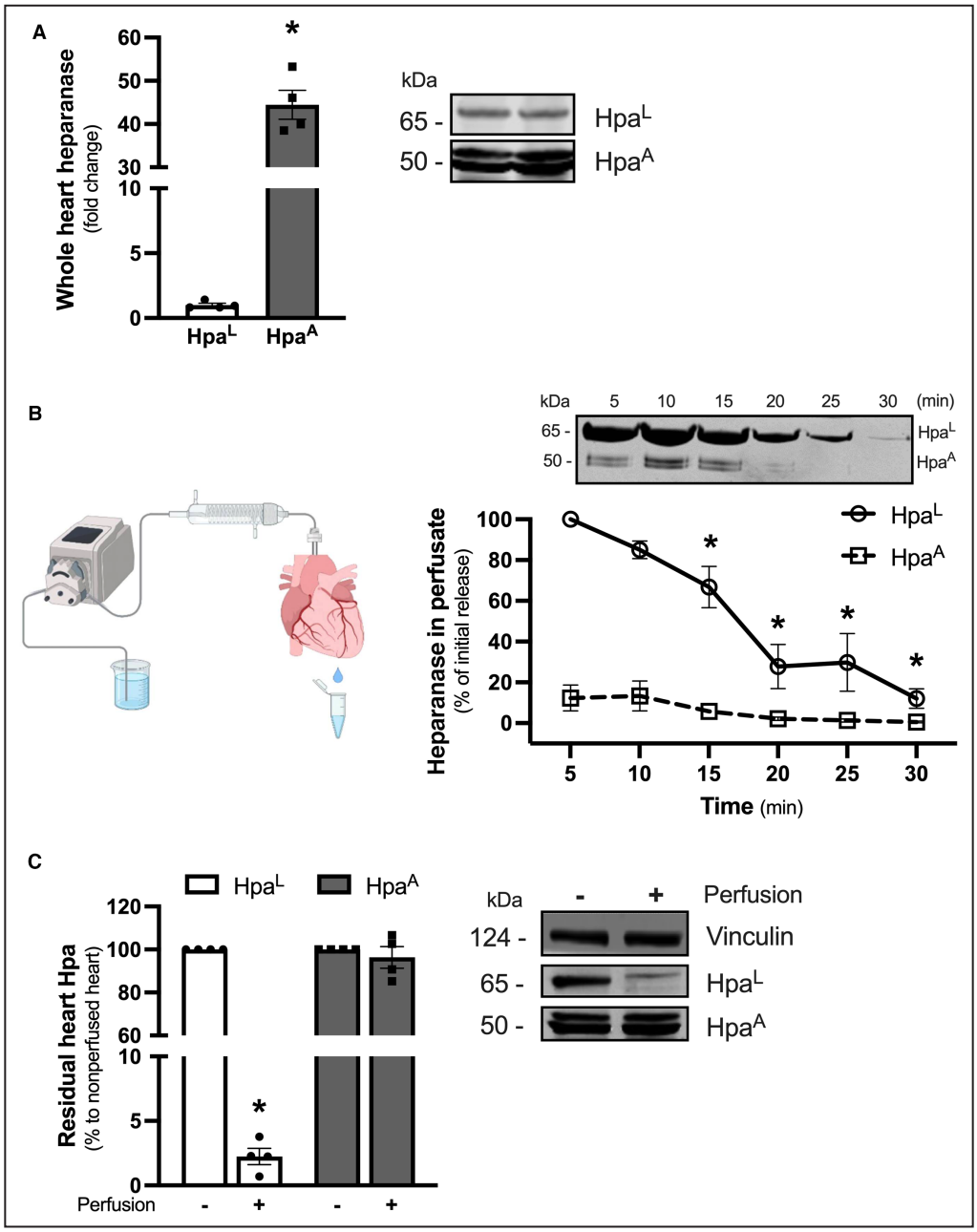

Figure 1. Differential expression of Hpa^{L} and Hpa^{A} in the heart and their secretory response to constant retrograde flow.

A, Hearts were excised from control rats and following tissue lysis and centrifugation, the supernatants were used to analyze both Hpa^{L} and Hpa^{A} using Western blot. *Significantly different from Hpa^{L}. **B**, Isolated hearts were cannulated via the aorta and a peristaltic pump used to retrogradely perfuse the coronary blood vessels (8 mL/min). The coronary effluent was collected over a period of 30 minutes at 1-minute intervals (left panel); 500 μL from every 1-minute sample over 5 minute intervals were pooled and concentrated before being used for Western blot analysis of heparanase. The release of heparanase over time was compared with the amount of Hpa^{L} secreted after the initial 5 minute perfusion (which was given a value of 100%; right panel); n=3. *Significantly different from the initial 5 minute Hpa^{L} sample. **C**, Following perfusion for 30 minutes, the hearts were collected and probed for residual heparanase expression. *Significantly different from the nonperfused heart. All data are presented as mean±SEM; *P<0.05 by the Student t-test (**A** and **C**) and 1-way ANOVA with Bonferroni post hoc test (**B**). Hpa^{A} indicates active heparanase; Hpa^{L}, latent heparanase.

heparanase forms (Figure 3C). Noteworthy, this secretory response into the medium was more apparent for Hpa^{L} compared with Hpa^{A} (Figure 3C). As purinergic receptor stimulation is known to cause activation of PKD,[34] a kinase that assists in vesicular transport of proteins from the Golgi to the plasma membrane,[35] we

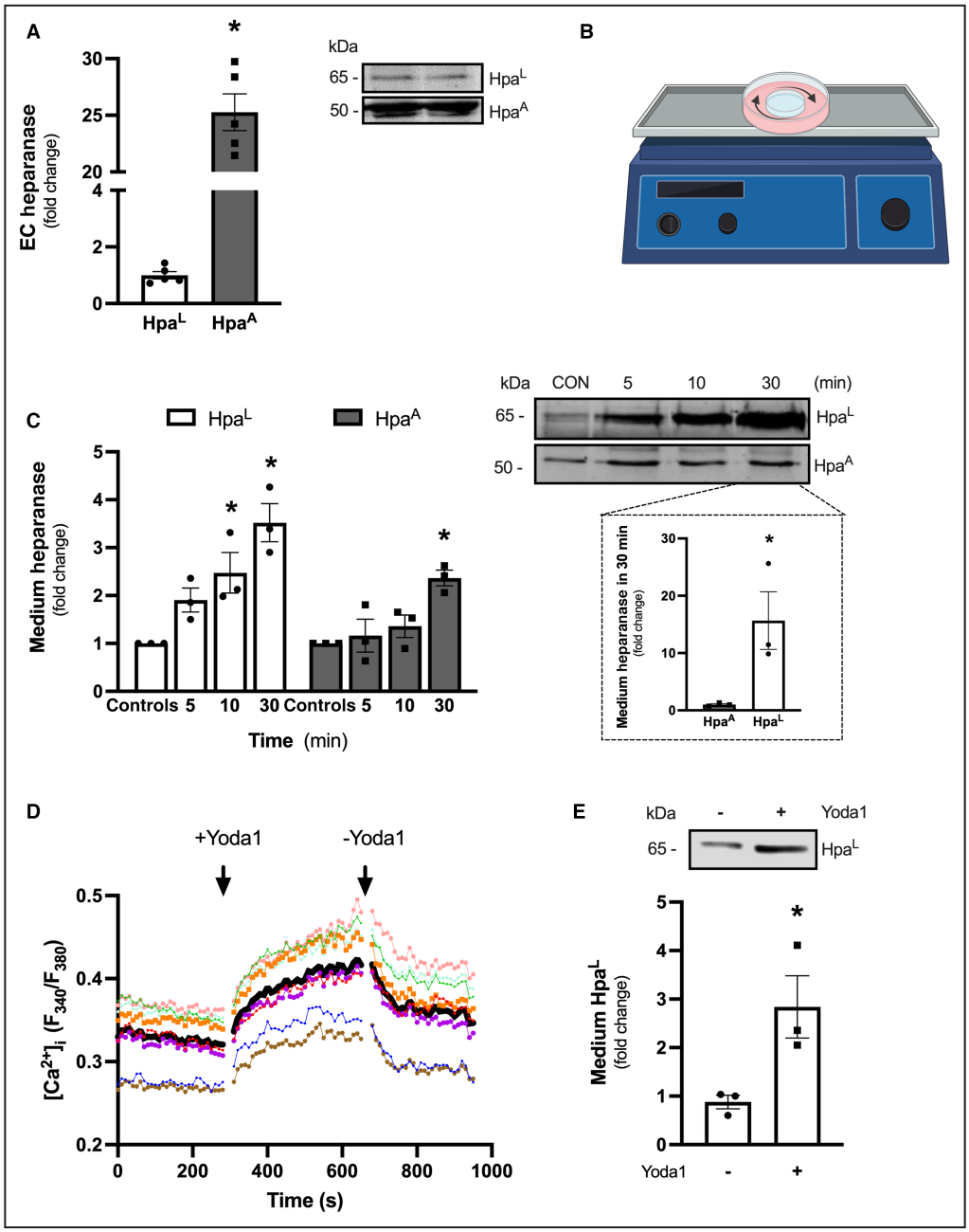

Figure 2. Expression of latent heparinase (Hpa^{L} and Hpa^{A} in ECs and their secretory response to laminar flow.

A, The EC lysates were collected to analyze both Hpa^{L} and Hpa^{A} using Western blot. *Significantly different from Hpa^{L}. **B**, A 100-mm culture dish was modified by attaching a 60-mm plate at its center. ECs were grown in the periphery of the larger plate until confluency. **C**, Following orbital shaking for 0 to 30 minutes at 250 rpm (≈15 dynes/cm^2), the medium was isolated, concentrated, and analyzed for heparanase secretion. Results were compared with cells kept under static condition for 30 minutes (control). Right inset depicts the comparative release of Hpa^{A} and Hpa^{L} in response to 30 minutes of LF. Left panel: *Significantly different from the static condition. Right inset: *Significantly different from Hpa^{A}. **D**, ECs were stained with Fura-2-AM and exposed to 1 μmol/L Yoda1 (a Piezo1 agonist). The experiment depicts 10 different regions in plain view to illustrate response heterogeneity (colored lines), with the black line depicting the average. The experiment was repeated 3 different times. **E**, ECs were exposed to 1 μmol/L Yoda1 for 60 minutes, and medium was collected, concentrated and analyzed by Western blot. *Significantly different from the control. All data are presented as mean±SEM; *P <0.05 by the Student t-test (**A**, **C** *inset* and **E**) and 1-way ANOVA with Bonferroni post hoc test (**C**). EC indicates endothelial cells; Hpa^{A}, active heparanase; Hpa^{L}, latent heparanase; and LF, laminar flow.

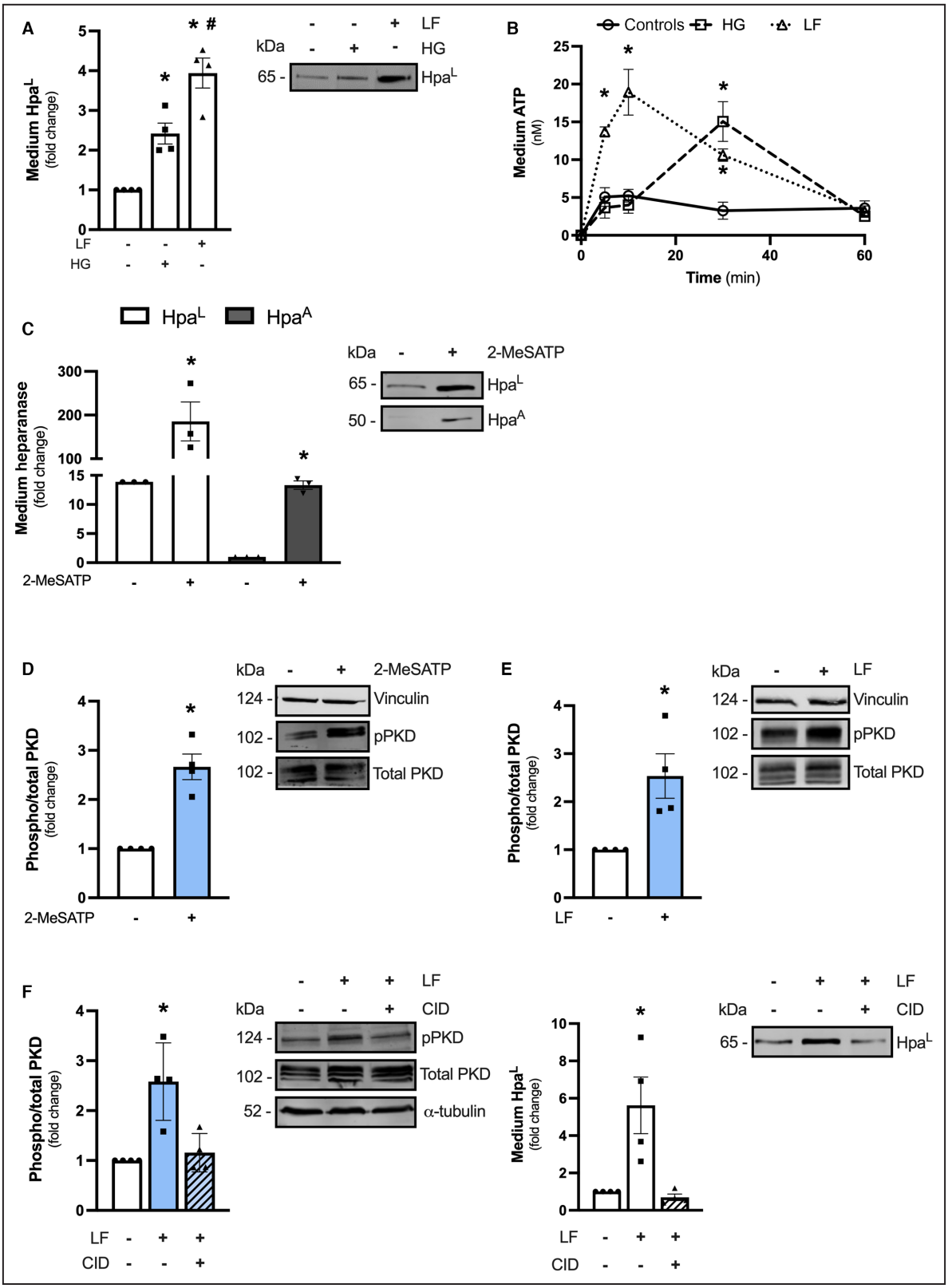

assessed PKD phosphorylation subsequent to exposure of ECs to 2-MeSATP. As hypothesized, these cells exhibited significantly higher PKD phosphorylation following 2-MeSATP treatment (Figure 3D), an effect that was reproduced in ECs subjected to LF (Figure 3E). Inhibition of PKD using CID-755673 (Figure 3F, *left panel*) prevented LF-induced heparanase secretion (Figure 3F, *right* panel). More importantly, Piezo1

Figure 3. Mechanosensitive response of ECs to secretion of heparanase.
A, The response of the EC to release heparanase after LF was compared with the effects of high glucose (25 mmol/L). After 30 minutes of either static with 5.5 mmol/L glucose, LF, or high glucose, the medium was collected, concentrated, and analyzed by Western blot. *Significantly different from the static control condition; #Significantly different from high glucose. **B**, Medium ATP secretion was measured using medium samples from ECs exposed to high glucose or LF; n=4. *Significantly different from the static control condition. **C**, ECs were treated with 100 μmol/L of the nonhydrolysable ATP analog (2-MeSATP) for 30 minutes and the medium collected for determination of Hpa^L and Hpa^A release. *Significantly different from the control condition. **D**, ECs were treated with 2-MeSATP for 30 minutes, and the lysates analyzed for phosphorylation of PK. *Significantly different from control. **E**, ECs exposed to LF for 30 minutes were analyzed for pPKD. *Significantly different from cells under static condition. **F**, ECs were treated with 10 μmol/L of CID for 30 minutes, followed by 30 minutes of LF. Cell lysates were collected for determination of PKD (left panel) and medium for analysis of Hpa^L secretion (right panel), respectively. *Significantly different from cells under static conditions without CID. All data are presented as mean±SEM; *$P<0.05$ by 1-way ANOVA with Bonferroni post hoc test (**A** and **F**) and the Student *t*-test (**B** through **E**). CID indicates PKD inhibitor CID-755673; EC, endothelial cells; HG, high glucose; Hpa^A, active heparanase; Hpa^L, latent heparinase; LF, laminar flow; 2-MeSATP, 2-methylthioadenosine 5′-triphosphate; and PKD, protein kinase D.

activation via Yoda1 also caused ATP release and activation of PKD (Figure S7A and B). Our data suggest that LF promotes secretion of EC heparanase through its modulation of the purinergic receptor.

CatL Activity Is Responsive to Flow-Mediated Regulation in ECs

Following its activation in lysosomes, the cysteine protease CatL catalyzes the conversion of enzymatically inactive Hpa^L into active Hpa^A[36] (Figure 4A, *left panel*). Here, we confirmed this effect and report that in the presence of CatL, Hpa^L is indeed converted into Hpa^A (Figure 4A, *right panel illustrating a representative blot*). As LF preferentially stimulates Hpa^L secretion from ECs, we postulated that a mechanism must exist to replenish Hpa^L following its depletion. Indeed, we report for the first time that in response to LF there was a time-dependent decline in CatL activity (Figure 4B, *left panel*), with a significant reduction observed at 4 hours (Figure 4B, *right panel*). Intriguingly, a decrease in CatL activity was also replicated in ECs exposed to HG (Figure 4C) and 2-MeSATP (Figure 4D). Our data suggest that in addition to its ability to promote the release of heparanase, LF is capable of increasing Hpa^L availability through its modification of CatL activity.

Hpa^A and Hpa^L Have Divergent Effects on Cardiomyocyte LPL

Vascular ECs and the underlying cardiomyocytes can communicate using crosstalk to affect cardiac metabolism.[37] We tested the ability of both forms of heparanase to release cardiomyocyte LPL for its onward relocation to the vascular lumen. Within 30 minutes, Hpa^A, but not Hpa^L, released cardiomyocyte LPL into the incubation medium (Figure 5A). We replicated this effect using myocytes that were incubated with concentrated perfusate fractions from the heart (P^{Fr}) containing both heparanase forms (Figure 5A). It should be noted that both Hpa^A and P^{Fr} only liberated a fraction of the cardiomyocyte HSPG-bound LPL compared with the amount released by ionic displacement using heparin (Figure 5A, *inset*). We also tested the ability of Hpa^L and Hpa^A to replenish cardiomyocyte LPL once it was released by heparin. Intriguingly, within 2 hours, only Hpa^L and the P^{Fr} accelerated LPL replenishment (Figure 5B). LPL movement to the cardiomyocyte surface HSPG requires actin cytoskeleton rearrangement, a process governed by activation of p38MAPK.[38] Measurement of this kinase following the LPL replenishment experiment showed its activation in response to Hpa^L and P^{Fr}, but not to Hpa^A (Figure 5C), with a corresponding increase in the F-G actin ratio (Figure 5D). As an activator of this kinase, thrombin (Figure 5E, *left panel*) also accelerated LPL replenishment (Figure 5E, *right panel*), likely through nuclear translocation of activated p38MAPK (Figure S8A) followed by HSP25 phosphorylation (Figure S8B). Our data suggest that flow-induced secreted heparanase can influence cardiac metabolism by increasing cardiomyocyte LPL displacement (Hpa^A) along with subsequent replenishment (Hpa^L).

Flow-Induced Heparanase Secretion Is Augmented Following Acute Diabetes

To test the impact that diabetes has on flow-mediated heparanase release from the heart, animals were made diabetic with streptozotocin. Four days after administration of streptozotocin, the animals exhibited both hyperglycemia and hypoinsulinemia (Figure 6A). Measurement of the heparin-releasable pool of LPL at the coronary lumen was augmented in the diabetic heart (Figure 6B *and inset*) and was unrelated to the total protein expression of heparanase (Figure 6C). Nevertheless, when hearts were perfused retrogradely, the diabetic hearts released significantly higher amounts of both forms of heparanase within the first 5 minutes (Figure 6D). As a result, these diabetic hearts also exhibited faster depletion of the releasable pool of heparanase (*data not shown*). Intriguingly, in ECs exposed to HG for 24 hours, Piezo1 showed increased expression (Figure 6E) and also the highest amount of Hpa^L secretion in response to LF (Figure 6F). This

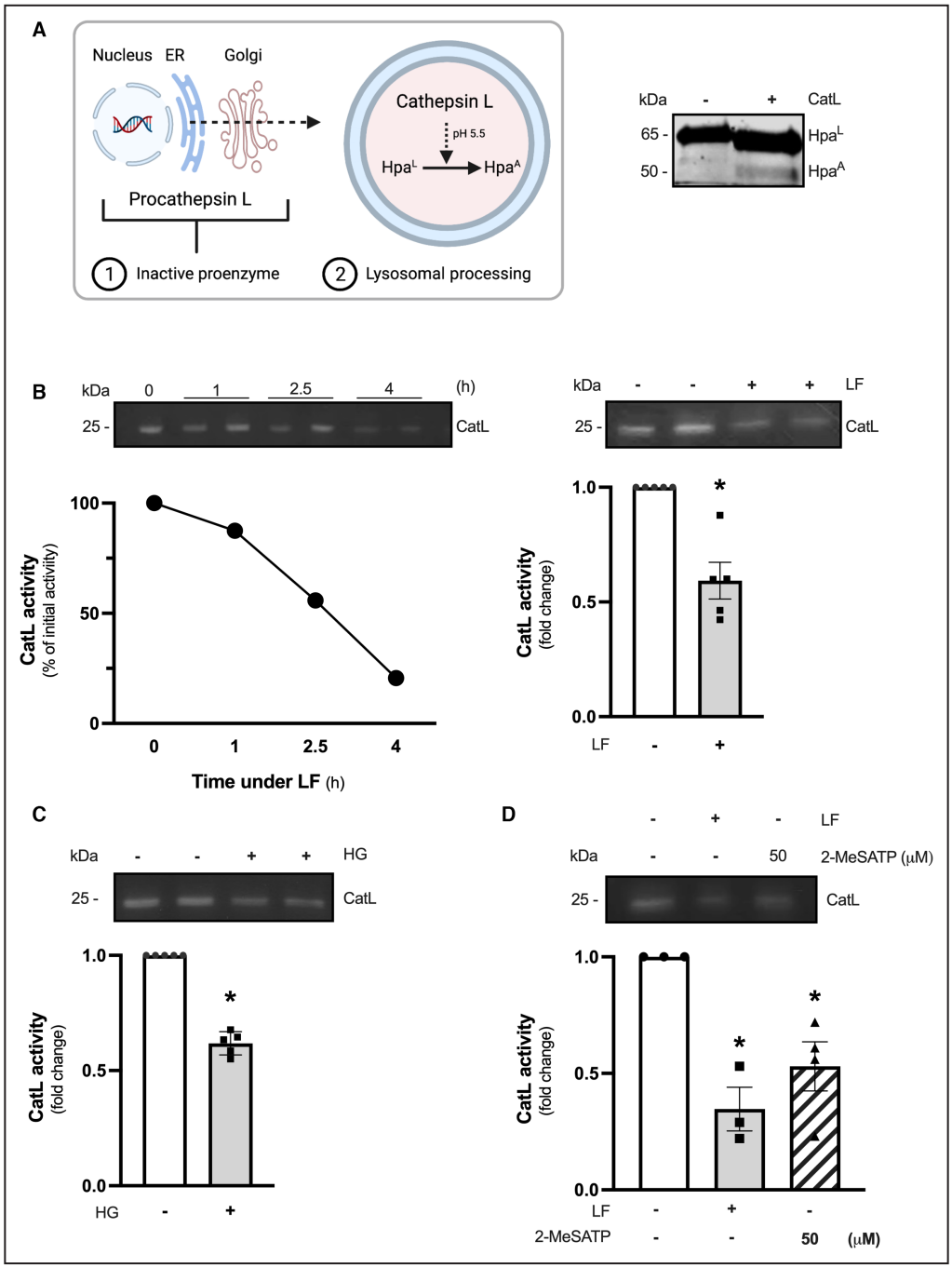

Figure 4. Laminar flow regulation of CatL activity in ECs.
A, An acidic pH is required for activation of CatL, allowing for the conversion of latent heparanase to active heparanase (left panel). Recombinant latent heparanase (200 ng) was incubated with or without recombinant cathepsin L (0.3 μg/μL) for 1 hour (37 °C in 100 mmol/L sodium acetate buffer, pH 5.5), and blotted against heparanase (right panel). **B**, ECs were exposed to laminar flow for 1 to 4 hours, lysates collected and subsequently assayed for CatL activity via zymography (representative figure, left panel). The right panel compares CatL activity in static vs laminar flow at 4 hours. *Significantly different from cells under static/control conditions. **C**, ECs were treated with or without high glucose (25 mmol/L) for 30 minutes and CatL activity determined by zymography. *Significantly different from cells under static/control conditions. **D**, ECs were treated with 50 μmol/L of 2-MeSATP for 4 hours. Lysates were analyzed for CatL activity using zymography and compared with ECs in the presence or absence of laminar flow. *Significantly different from cells under static control conditions. All data are presented as mean±SEM. *P<0.05 by the Student t-test (**B** and **C**) and 1-way ANOVA with Bonferroni post hoc test (**D**). 2-MeSATP indicates 2-methylthioadenosine 5′-triphosphate; CatL, cathepsin L; EC, endothelial cells; ER, endoplasmic reticulum; HG, high glucose; Hpa^A, active heparanase; Hpa^L, latent heparanase; LF, laminar flow; and rCatL, recombinant cathepsin L.

change in Piezo1 expression was observed as early as 4 hours after incubation with HG (Figure S9). The osmotic control, mannitol, did not increase Piezo1 expression (Figure S10). Our data imply that the mechanosensitive release of heparanase and its effect on LPL could be an additional mechanism to explain the augmented substrate preference of the diabetic heart towards LPL-derived FAs.

DISCUSSION

The aim of the present study was to identify the physiological processes controlling the metabolic network that generates energy for cardiac contraction. Our intention was to understand the crosstalk between ECs and cardiomyocytes, 2 cell types that work together to deliver FA, an important fuel for production of energy in the heart. Overall, we conclude that on sensing fluid shear stress, the EC communicates this information to subjacent cardiomyocytes, and does so with the help of EC heparanase. This process of mechanotransduction is altered following diabetes to offer a unique and effective way to support the reliance of the diabetic heart on FAs.

For its beat-to-beat contraction, one major substrate that provides the heart its constant demand for energy is FA, provided by a number of different pathways including LPL. For the heart to use this energy substrate from LPL, this enzyme requires translocation from cardiomyocytes to the vascular lumen, an action achieved by heparanase.[12] It is Hpa^A, by its cleavage of HS side chains on cardiomyocyte HSPG, that liberates LPL for its onward movement.[13] Given this important function for Hpa^A, the heart would require an existing cytosolic storage pool of Hpa^A rather than de novo synthesis when there is an immediate demand for FA. Indeed, our results of ≈40-fold higher amount of Hpa^A compared with Hpa^L supports the value of the enzymatic action of Hpa^A in LPL transfer. Despite this overabundant storage depot of Hpa^A, it appeared that LF was only capable of inducing a partial discharge into the perfusate and this was likely from a distinctive subset pool that is readily releasable. It should be noted that the limited discharge of Hpa^A in response to flow could be considered practical to avoid excessive FA delivery, in addition to superfluous HS side chain cleavage, leading to cardiac remodeling and hypertrophy.[39–41] Additionally, when extrapolated to the in vivo condition, this released amount of Hpa^A would be even smaller as it only would be responsive to LF in diastole, unlike the retrograde coronary perfusion that was used to release heparanase from the ex vivo heart under unrelenting constant flow for 30 minutes—a limitation of the Langendorff heart model. Interestingly, despite the comparatively lower amount of intracellular Hpa^L, this form was more responsive to flow-induced release compared with Hpa^A. This preference for Hpa^L release may itself have multiple implications including (1) cellular reuptake for lysosomal conversion into Hpa^A,[15,16] (2) ionic binding and controlled release of HSPG-bound growth factors like vascular endothelial growth factors,[42] and (3) activation of intracellular signaling in subjacent cells to promote protein secretion[12] and cell survival.[43,44]

In studying the cellular origins of flow-mediated heparanase release from isolated hearts, we determined that of the 2 forms of heparanase in ECs (that make up ≈45% of cells in the heart[45]), there was a greater amount of Hpa^A compared with Hpa^L. As this distribution mimicked results from the whole heart, we selected ECs to examine flow-induced heparanase release. Using orbital rotation of medium over a monolayer of ECs,[26] we first confirmed that this model was indeed demonstrative of laminar shear stress. Importantly, in response to LF, and similar to the whole heart perfusion, there was a rapid and incremental release of heparanase, with Hpa^L being the dominant form released. As this effect of LF was replicated by specific activation of the mechanosensitive ion channel Piezo1, our data for the first time suggest that flow-induced heparanase release from ECs may be an important mechanical regulator of cardiac energy metabolism.

Similar to LF, we have previously shown that the EC is also responsive to glucose-induced heparanase secretion, through a mechanism that includes ATP release and purinergic receptor activation.[33] We compared the amount of heparanase released by LF and HG and demonstrated that LF was a more robust and earlier signal for releasing both Hpa^L and Hpa^A over HG. This distinction could be the consequence of an earlier release of ATP with LF compared with HG. A possible explanation for this effect is that LF applied to ECs rapidly augments mitochondrial ATP generation, whereas HG generates ATP through glycolysis, the former being a greater source of ATP than the latter.[11,23] Given that HG and LF-mediated mechanosignaling linked heparanase secretion to ATP release, we used 2-MeSATP, a nonhydrolysable ATP analog that acts as a P2Y receptor agonist, and observed a robust increase in both Hpa^L and Hpa^A secretion. Interestingly, one downstream effect of purinergic receptor activation in glial cells is a rapid increase in PKD phosphorylation and activity,[34] an effect that was replicated in our study where ECs were exposed to 2-MeSATP, LF, and Yoda1. PKD is known to regulate fission of vesicles from the Golgi membranes followed by their movement to the plasma membrane for eventual extracellular secretion.[46] As a PKD-specific inhibitor prevented LF-mediated PKD phosphorylation and heparanase release, our data suggest that LF, through mechanosignaling and purinergic receptor activation, facilitates Golgi transport and packaging of Hpa^L into endocytic vesicles for secretion.[47]

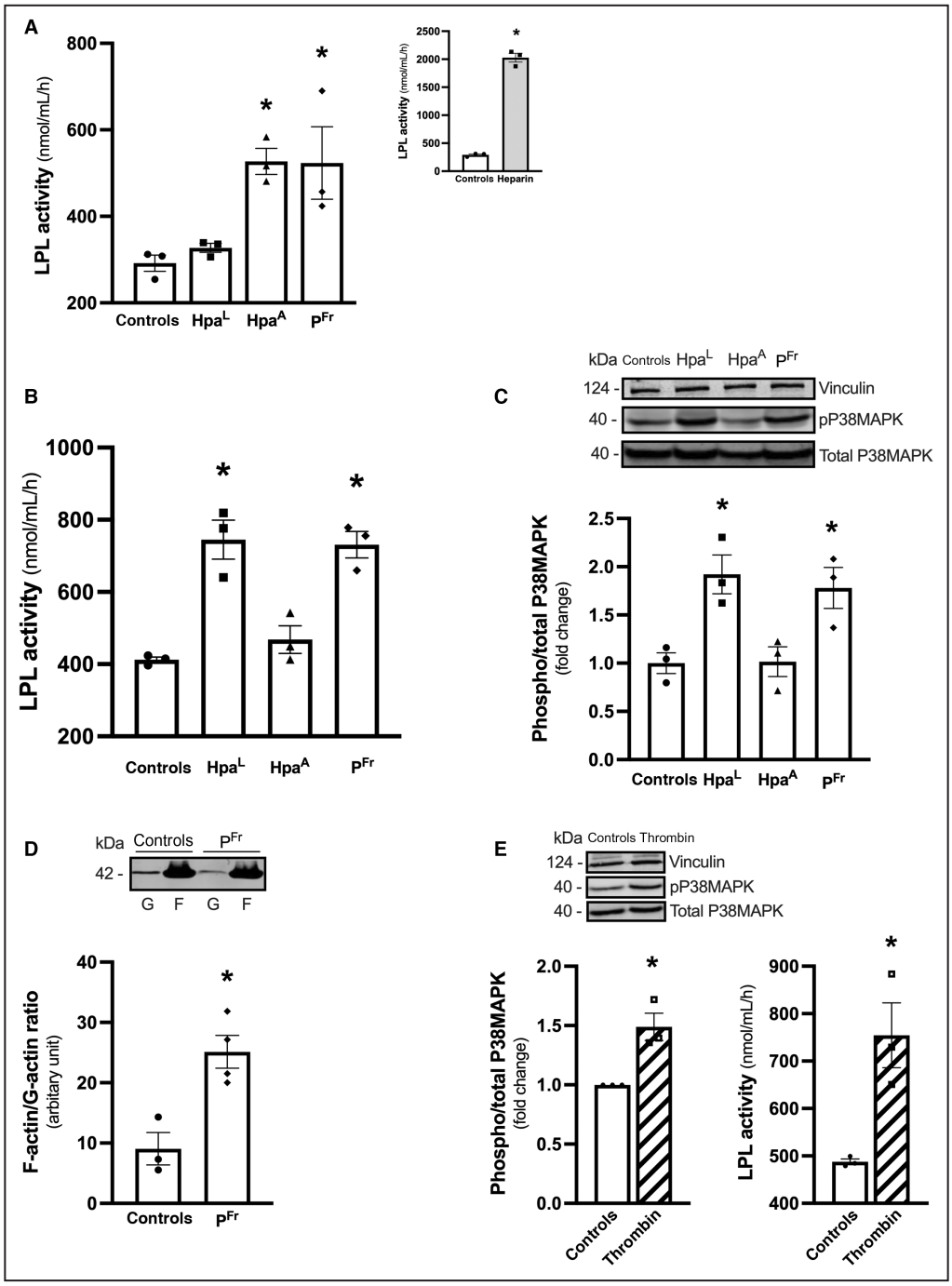

In addition to its effect on EC heparanase secretion, we also tested whether LF modulates heparanase availability, especially Hpa^L which is the dominant form released. It should be noted that conversion of the 65-kDa Hpa^L into the 50-kDa Hpa^A occurs within lysosomes through the action of a protease, CatL.[48] For its optimal activity, CatL requires a reducing and an acidic environment of ~pH 5.5.[27,49] This acidic pH is regulated by the V-ATPase proton pump whereby H^+ ions are pumped into the endosome/lysosome via ATP hydrolyzation.[50] Within lysosomes, CatL cleaves and excises the 6-kDa linker at Gln_{157}-Lys_{158} of heparanase, resulting in an 8-kDa and 50-kDa heterodimer active form.[51,52] Investigation of CatL with respect to heparanase modulation indicated that the EC response to LF, HG, or 2-MeSATP did not change CatL protein levels but rather resulted in a decrease in CatL activity through mechanisms that are currently undetermined. Interestingly, in mouse aortic EC,[27] unidirectional shear-stress also decreased CatL activity, suggesting that this protease is mechanosensitive. One possibility is that as purinergic receptor

Figure 5. Effects of heparanase on release and replenishment of cardiomyocyte LPL.
A, Calcium-tolerant cardiomyocytes (4×10^5 cells/mL) were isolated and plated on laminin-coated 6-well plates. Recombinant latent heparanase and active heparanase (1 μg/mL) and perfusate fractions (20-μL per well) were added to each well and medium collected after 30 minutes for determination of LPL released from the cardiomyocyte cell surface. The inset describes LPL released from cardiomyocytes by heparin (2 U/mL). *Significantly different from control. **B**, Heparin (2 U/mL; 5 minutes) was first used to ionically detach cardiomyocyte cell surface LPL. Following washing to remove any residual heparin, cells were treated with recombinant latent heparanase and active heparanase (1 μg/mL) and perfusate fractions (20-μL per well) for 2 hours. After this, the treatment medium was replaced and a second heparin incubation performed to quantify the amount of LPL replenished at the cell surface for 2 hours. *Significantly different from control. **C**, Following LPL replenishment after 2 hours, the cell lysates of cardiomyocytes were collected and analyzed for P38MAPK using Western blot. *Significantly different from control. **D**, Cardiomyocytes were treated with perfusate fractions for 2 hours and used for determination of F–/G-actin ratio. Total actin was centrifuged to isolate F-actin (pellet) and G-actin (supernatant). The ratio of F–/G-actin was determined using Western blot and imaged and quantified by Licor. An increase in the ratio of F–/G-actin represents polymerization of actin filaments. *Significantly different from control. **E**, The effect of thrombin to influence LPL replenishment was also tested. After the initial heparin incubation, cells were incubated with thrombin (0.05 U/mL) for 2 hours. A second heparin incubation was used to determine the amount of LPL replenished (*left panel*). Phosphorylation of p38MAPK was confirmed in the cell lysates (*right panel*). *Significantly different from control. All data are presented as mean±SEM; *P<0.05 by one-way ANOVA with Bonferroni post hoc test (**A** through **C**) and the Student t-test (**D** and **E**). Hpa^A indicates active heparanase; Hpa^L, latent heparanase; LPL, lipoprotein lipase; P^{Fr}, perfusate fractions; P38MAPK, P38-mitogen activated protein kinase; and pP38MAPK, phospho-P38-mitogen activated protein kinase.

activation is known to elevate lysosomal pH with Ca^{2+} influx,[53] this would limit maturation of CatL and therefore its activity. Our data suggest that in addition to its release following LF, heparanase is modulated by an intracellular noncanonical mechanism whereby reduced CatL activity would allow for more Hpa^L availability to offset its higher secretion.

Present on the cardiomyocyte cell surface is a pool of LPL that once released, moves to the vascular lumen to breakdown circulating triglyceride.[13] Release of LPL from this cell surface pool was apparent with Hpa^A (that is known to cleave HS side chains of HSPG) and also with P^{Fr} that contain Hpa^A. When compared with heparin, which displaces LPL through ionic interaction with the enzyme, the Hpa^A effect on LPL release was substantially lower and could be related to the amount of enzyme used or the time required for its enzymatic activity. Once released, the mechanism which reloads this surface cardiomyocyte LPL is undefined and could be related to transmembrane signaling initiated by Hpa^L-induced clustering of HSPG.[54] Interestingly, the heparin binding region (Lys_{158}- Asp_{171}) on Hpa^L has proadhesive properties that can physically induce HSPG clustering and downstream signaling, including p38MAPK which is pivotal for actin cytoskeleton reorganization.[16,19,20,55–58] Intriguingly, both Hpa^L and P^{Fr} moved intracellular LPL to replenish the released reservoir, an effect that likely involved p38MAPK activation. This effect was replicated using thrombin, confirming the distinct role of Hpa^L in p38MAPK-mediated LPL replenishment. This would allow vesicles containing LPL to move along the actin filament network and eventually bind to HSPG on the plasma membrane.[38] Overall, our data suggest that the initial cropping of HS by Hpa^A (releasing cardiomyocyte LPL and generating HS ends that are permissive for aggregation) could be followed by Hpa^L induced clustering (to promote reloading of LPL).

As glucose uptake and oxidation are impaired in diabetes, the heart is obliged to use FA almost exclusively.[1,3] Multiple mechanisms operate to make this achievable including augmented adipose tissue lipolysis, greater hepatic very-low-density lipoprotein-triglyceride availability,[59] increase in cardiac FA transporters,[60] enhanced adipose triglyceride lipase breakdown of stored cardiomyocyte triglyceride to FA[61] and increased luminal LPL that initiates lipolysis of lipoproteins.[62] Indeed, in response to acute streptozotocin diabetes, this and our previous studies[62–64] report that LPL is "switched on", causing a robust expansion of coronary LPL activity. This increase in vascular LPL was unrelated to the amount of heparanase, as control and diabetic hearts displayed identical expression of both forms of heparanase. However, we report for the first time that retrograde perfusion of the diabetic heart releases significantly higher amounts of Hpa^L and Hpa^A, an effect that could be ascribed to an increase in Piezo1 expression. Indeed, when whole blood was incubated with HG, the expression of Piezo1 increased,[65] an effect that was also seen when we incubated EC in HG. Even more compelling was the response of these HG-exposed ECs to LF. These ECs demonstrated an exaggerated heparanase release similar to when diabetic hearts are exposed to constant perfusion, an effect that may explain the augmented LPL in these hearts. Altogether, our data highlight a novel and unsuspected role for augmented LF-induced heparanase release to accelerate LPL translocation in diabetic hearts.

In conclusion, this study reports on the ability of EC to sense fluid shear stress and communicate this information to subjacent cardiomyocytes with the help of heparanase. This flow-induced mechanosensing and its dynamic control of cardiac metabolism to generate ATP, using LPL-derived FAs, is exquisitely adapted to respond to disease conditions, like diabetes (Figure S11).

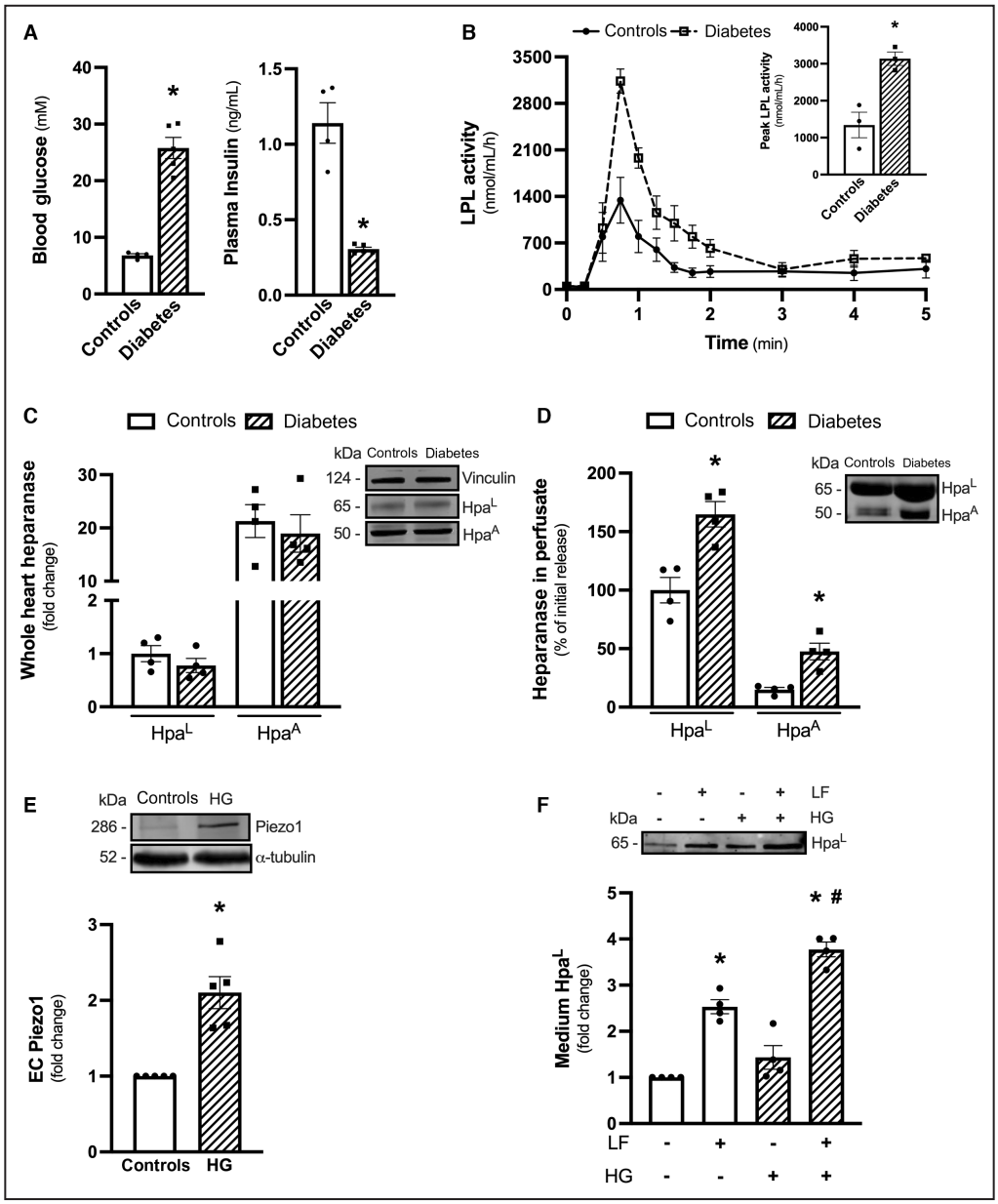

Figure 6. In vivo and in vitro effect of high glucose on flow-induced heparanase release.
A, Animals were made diabetic with 55 mg/kg streptozotocin (diabetes). After 4 days, hyperglycemia was confirmed in tail-tip blood samples using a glucometer and glucose test strips (left panel). At termination, hearts were exsanguinated and blood in the thoracic cavity collected for determination of plasma insulin using an ELISA (right panel). *Significantly different from control. **B**, Hearts from control and diabetic animals were perfused with heparin (5 U/mL), and coronary effluent over 5 minutes was collected for determination of LPL activity; n=3. The inset illustrates only peak LPL activity. *Significantly different from control. **C**, Hearts were excised from control and diabetic rats to analyze both latent heparanase and active heparanase using Western blot. **D**, Isolated hearts were perfused retrogradely, and the coronary effluent was collected over a period of 30 minutes at 1-minute intervals. 500 μL from the first 5 minutes intervals was pooled and concentrated for Western blot analysis of heparanase. *Significantly different from control. **E**, ECs were exposed to 5 mmol/L (control) or 25 mmol/L glucose (high glucose) for 24 hours and analyzed for Piezo1 expression. *Significantly different from control. **F**, ECs were exposed to 5 or 25 mmol/L glucose for 24 hours before the experiment. Following a wash, the cells were either put under static or LF conditions for 30 minutes, and medium collected for determination of latent heparanase release. *Significantly different from static; #Significantly different from LF. All data are presented as mean±SEM; *P<0.05 by the Student t-test (**A** and **E**) and 1-way ANOVA with Bonferroni post hoc test (**D** and **F**). EC indicates endothelial cells; HG, high glucose; Hpa^A, active heparanase; Hpa^L, latent heparanase; LF, laminar flow; and LPL, lipoprotein lipase.

Limitations

Although ECs and cardiomyocytes make up ≈75% of the cells present in the heart,[45] with cardiomyocytes expressing no *heparanase*, we suggested that the majority of heparanase secreted from the whole heart in response to LF arises from ECs. Whether cardiac fibroblasts can also contribute to flow-mediated heparanase release is currently unknown.

ARTICLE INFORMATION

Received August 29, 2022; accepted October 12, 2022.

Affiliations

Faculty of Pharmaceutical Sciences, UBC, Vancouver, British Columbia, Canada (C.S.L., Y.Z., R.S., T.W., B.H., B.R.); Department of Cellular and Physiological Sciences & Department of Surgery, Diabetes Focus Team, Life Sciences Institute, UBC, Vancouver, British Columbia, Canada (A.J.M., H.H.C., J.D.J.); and Cancer and Vascular Biology Research Center, Rappaport Faculty of Medicine, Technion, Haifa, Israel (I.V.).

Acknowledgments

Mr Lee was involved with all data generation and collation and writing the paper with Dr Rodrigues. Ms Zhai performed the zymography experiments. Ms Shang set up the isolated heart perfusion system to determine heparanase secretion. Mr Wong contributed towards the Western blotting of numerous proteins. Ms Mattison, Mr Cen, and Dr Johnson helped with the calcium measurements. Dr Vlodavsky generated the Hpa^{L-} and Hpa^{A-}. Ms Hussein oversaw the entire project and contributed to the editing of the manuscript. Mr Lee and Dr Rodrigues generated the hypothesis, designed the study, and wrote the manuscript. Dr Rodrigues is the guarantor of this study.

Sources of Funding

This work was supported by operating grants from the Canadian Institutes of Health Research [PJT-178134] and the Heart and Stroke Foundation of Canada [G-19-0026493]. Dr Brian Rodrigues is the guarantor of this study.

Disclosures

The figures in this article were created with Biorender.com.

Supplemental Material

Figure S1–S11

REFERENCES

1. Lopaschuk GD, Ussher JR, Folmes CD, Jaswal JS, Stanley WC. Myocardial fatty acid metabolism in health and disease. *Physiol Rev*. 2010;90:207–258. doi: 10.1152/physrev.00015.2009
2. Murashige D, Jang C, Neinast M, Edwards JJ, Cowan A, Hyman MC, Rabinowitz JD, Frankel DS, Arany Z. Comprehensive quantification of fuel use by the failing and nonfailing human heart. *Science*. 2020;370:364–368. doi: 10.1126/science.abc8861
3. An D, Rodrigues B. Role of changes in cardiac metabolism in development of diabetic cardiomyopathy. *Am J Physiol Heart Circ Physiol*. 2006;291:H1489–H1506. doi: 10.1152/ajpheart.00278.2006
4. Kim MS, Wang Y, Rodrigues B. Lipoprotein lipase mediated fatty acid delivery and its impact in diabetic cardiomyopathy. *Biochim Biophys Acta*. 2012;1821:800–808. doi: 10.1016/j.bbalip.2011.10.001
5. Eckel RH. Lipoprotein lipase. A multifunctional enzyme relevant to common metabolic diseases. *N Engl J Med*. 1989;320:1060–1068. doi: 10.1056/NEJM198904203201607
6. Enerback S, Gimble JM. Lipoprotein lipase gene expression: physiological regulators at the transcriptional and post-transcriptional level. *Biochim Biophys Acta*. 1993;1169:107–125. doi: 10.1016/0005-2760(93)90196-g
7. Iozzo RV, San Antonio JD. Heparan sulfate proteoglycans: heavy hitters in the angiogenesis arena. *J Clin Invest*. 2001;108:349–355. doi: 10.1172/JCI13738
8. Allan CM, Larsson M, Jung RS, Ploug M, Bensadoun A, Beigneux AP, Fong LG, Young SG. Mobility of "HSPG-bound" LPL explains how LPL is able to reach GPIHBP1 on capillaries. *J Lipid Res*. 2017;58:216–225. doi: 10.1194/jlr.M072520
9. Young SG, Davies BS, Voss CV, Gin P, Weinstein MM, Tontonoz P, Reue K, Bensadoun A, Fong LG, Beigneux AP. GPIHBP1, an endothelial cell transporter for lipoprotein lipase. *J Lipid Res*. 2011;52:1869–1884. doi: 10.1194/jlr.R018689
10. Otarod JK, Goldberg IJ. Lipoprotein lipase and its role in regulation of plasma lipoproteins and cardiac risk. *Curr Atheroscler Rep*. 2004;6:335–342. doi: 10.1007/s11883-004-0043-4
11. Wan A, Rodrigues B. Endothelial cell-cardiomyocyte crosstalk in diabetic cardiomyopathy. *Cardiovasc Res*. 2016;111:172–183. doi: 10.1093/cvr/cvw159
12. Wang F, Kim MS, Puthanveetil P, Kewalramani G, Deppe S, Ghosh S, Abrahani A, Rodrigues B. Endothelial heparanase secretion after acute hypoinsulinemia is regulated by glucose and fatty acid. *Am J Physiol Heart Circ Physiol*. 2009;296:H1108–H1116. doi: 10.1152/ajpheart.01312.2008
13. Wang Y, Zhang D, Chiu AP, Wan A, Neumaier K, Vlodavsky I, Rodrigues B. Endothelial heparanase regulates heart metabolism by stimulating lipoprotein lipase secretion from cardiomyocytes. *Arterioscler Thromb Vasc Biol*. 2013;33:894–902. doi: 10.1161/ATVBAHA.113.301309
14. Bame KJ. Heparanases: endoglycosidases that degrade heparan sulfate proteoglycans. *Glycobiology*. 2001;11:91R–98R. doi: 10.1093/glycob/11.6.91r
15. Fairbanks MB, Mildner AM, Leone JW, Cavey GS, Mathews WR, Drong RF, Slightom JL, Bienkowski MJ, Smith CW, Bannow CA, et al. Processing of the human heparanase precursor and evidence that the active enzyme is a heterodimer. *J Biol Chem*. 1999;274:29587–29590. doi: 10.1074/jbc.274.42.29587
16. Gingis-Velitski S, Zetser A, Kaplan V, Ben-Zaken O, Cohen E, Levy-Adam F, Bashenko Y, Flugelman MY, Vlodavsky I, Ilan N. Heparanase uptake is mediated by cell membrane heparan sulfate proteoglycans. *J Biol Chem*. 2004;279:44084–44092. doi: 10.1074/jbc.M402131200
17. Pikas DS, Li JP, Vlodavsky I, Lindahl U. Substrate specificity of heparanases from human hepatoma and platelets. *J Biol Chem*. 1998;273:18770–18777. doi: 10.1074/jbc.273.30.18770
18. Abboud-Jarrous G, Rangini-Guetta Z, Aingorn H, Atzmon R, Elgavish S, Peretz T, Vlodavsky I. Site-directed mutagenesis, proteolytic cleavage, and activation of human proheparanase. *J Biol Chem*. 2005;280:13568–13575. doi: 10.1074/jbc.M413370200
19. Fux L, Ilan N, Sanderson RD, Vlodavsky I. Heparanase: busy at the cell surface. *Trends Biochem Sci*. 2009;34:511–519. doi: 10.1016/j.tibs.2009.06.005
20. Cui H, Shao C, Liu Q, Yu W, Fang J, Yu W, Ali A, Ding K. Heparanase enhances nerve-growth-factor-induced PC12 cell neuritogenesis via the p38 MAPK pathway. *Biochem J*. 2011;440:273–282. doi: 10.1042/BJ20110167
21. Riaz A, Ilan N, Vlodavsky I, Li JP, Johansson S. Characterization of heparanase-induced phosphatidylinositol 3-kinase-AKT activation and its integrin dependence. *J Biol Chem*. 2013;288:12366–12375. doi: 10.1074/jbc.M112.435172
22. Schubert SY, Ilan N, Shushy M, Ben-Izhak O, Vlodavsky I, Goldshmidt O. Human heparanase nuclear localization and enzymatic activity. *Lab Invest*. 2004;84:535–544. doi: 10.1038/labinvest.3700084
23. Yamamoto K, Imamura H, Ando J. Shear stress augments mitochondrial ATP generation that triggers ATP release and Ca(2+) signaling in vascular endothelial cells. *Am J Physiol Heart Circ Physiol*. 2018;315:H1477–H1485. doi: 10.1152/ajpheart.00204.2018
24. Douguet D, Patel A, Xu A, Vanhoutte PM, Honore E. Piezo ion channels in cardiovascular mechanobiology. *Trends Pharmacol Sci*. 2019;40:956–970. doi: 10.1016/j.tips.2019.10.002
25. Sambandam N, Chen X, Cam MC, Rodrigues B. Cardiac lipoprotein lipase in the spontaneously hypertensive rat. *Cardiovasc Res*. 1997;33:460–468. doi: 10.1016/s0008-6363(96)00201-5
26. dela Paz NG, Walshe TE, Leach LL, Saint-Geniez M, D'Amore PA. Role of shear-stress-induced VEGF expression in endothelial cell survival. *J Cell Sci*. 2012;125:831–843. doi: 10.1242/jcs.084301
27. Platt MO, Ankeny RF, Jo H. Laminar shear stress inhibits cathepsin L activity in endothelial cells. *Arterioscler Thromb Vasc Biol*. 2006;26:1784–1790. doi: 10.1161/01.ATV.0000227470.72109.2b
28. Blich M, Golan A, Arvatz G, Sebbag A, Shafat I, Sabo E, Cohen-Kaplan V, Petcherski S, Avniel-Polak S, Eitan A, et al. Macrophage activation

by heparanase is mediated by TLR-2 and TLR-4 and associates with plaque progression. *Arterioscler Thromb Vasc Biol*. 2013;33:e56–e65. doi: 10.1161/ATVBAHA.112.254961
29. Narmoneva DA, Vukmirovic R, Davis ME, Kamm RD, Lee RT. Endothelial cells promote cardiac myocyte survival and spatial reorganization: implications for cardiac regeneration. *Circulation*. 2004;110:962–968. doi: 10.1161/01.CIR.0000140667.37070.07
30. Wang F, Jia J, Lal N, Zhang D, Chiu AP, Wan A, Vlodavsky I, Hussein B, Rodrigues B. High glucose facilitated endothelial heparanase transfer to the cardiomyocyte modifies its cell death signature. *Cardiovasc Res*. 2016;112:656–668. doi: 10.1093/cvr/cvw211
31. Jin YJ, Chennupati R, Li R, Liang G, Wang S, Iring A, Graumann J, Wettschureck N, Offermanns S. Protein kinase N2 mediates flow-induced endothelial NOS activation and vascular tone regulation. *J Clin Invest*. 2021;131:131. doi: 10.1172/JCI145734
32. Wang Q, More SK, Vomhof-DeKrey EE, Golovko MY, Basson MD. Small molecule FAK activator promotes human intestinal epithelial monolayer wound closure and mouse ulcer healing. *Sci Rep*. 2019;9:14669. doi: 10.1038/s41598-019-51183-z
33. Wang F, Wang Y, Kim MS, Puthanveetil P, Ghosh S, Luciani DS, Johnson JD, Abrahani A, Rodrigues B. Glucose-induced endothelial heparanase secretion requires cortical and stress actin reorganization. *Cardiovasc Res*. 2010;87:127–136. doi: 10.1093/cvr/cvq051
34. Carrasquero LM, Delicado EG, Sanchez-Ruiloba L, Iglesias T, Miras-Portugal MT. Mechanisms of protein kinase D activation in response to P2Y(2) and P2X7 receptors in primary astrocytes. *Glia*. 2010;58:984–995. doi: 10.1002/glia.20980
35. Kim MS, Wang F, Puthanveetil P, Kewalramani G, Hosseini-Beheshti E, Ng N, Wang Y, Kumar U, Innis S, Proud CG, et al. Protein kinase D is a key regulator of cardiomyocyte lipoprotein lipase secretion after diabetes. *Circ Res*. 2008;103:252–260. doi: 10.1161/CIRCRESAHA.108.178681
36. Abboud-Jarrous G, Atzmon R, Peretz T, Palermo C, Gadea BB, Joyce JA, Vlodavsky I. Cathepsin L is responsible for processing and activation of proheparanase through multiple cleavages of a linker segment. *J Biol Chem*. 2008;283:18167–18176. doi: 10.1074/jbc.M801327200
37. Shang R, Rodrigues B. Lipoprotein lipase and its delivery of fatty acids to the heart. *Biomolecules*. 2021;11:1016. doi: 10.3390/biom11071016
38. Kim MS, Kewalramani G, Puthanveetil P, Lee V, Kumar U, An D, Abrahani A, Rodrigues B. Acute diabetes moderates trafficking of cardiac lipoprotein lipase through p38 mitogen-activated protein kinase-dependent actin cytoskeleton organization. *Diabetes*. 2008;57:64–76. doi: 10.2337/db07-0832
39. Bayomy AF, Bauer M, Qiu Y, Liao R. Regeneration in heart disease-is ECM the key? *Life Sci*. 2012;91:823–827. doi: 10.1016/j.lfs.2012.08.034
40. Frangogiannis NG. The extracellular matrix in myocardial injury, repair, and remodeling. *J Clin Invest*. 2017;127:1600–1612. doi: 10.1172/JCI87491
41. Kardami E, Jiang ZS, Jimenez SK, Hirst CJ, Sheikh F, Zahradka P, Cattini PA. Fibroblast growth factor 2 isoforms and cardiac hypertrophy. *Cardiovasc Res*. 2004;63:458–466. doi: 10.1016/j.cardiores.2004.04.024
42. Zhang D, Wan A, Chiu AP, Wang Y, Wang F, Neumaier K, Lal N, Bround MJ, Johnson JD, Vlodavsky I, et al. Hyperglycemia-induced secretion of endothelial heparanase stimulates a vascular endothelial growth factor autocrine network in cardiomyocytes that promotes recruitment of lipoprotein lipase. *Arterioscler Thromb Vasc Biol*. 2013;33:2830–2838. doi: 10.1161/ATVBAHA.113.302222
43. Kivela R, Bry M, Robciuc MR, Rasanen M, Taavitsainen M, Silvola JM, Saraste A, Hulmi JJ, Anisimov A, Mayranpaa MI, et al. VEGF-B-induced vascular growth leads to metabolic reprogramming and ischemia resistance in the heart. *EMBO Mol Med*. 2014;6:307–321. doi: 10.1002/emmm.201303147
44. Zhang F, Tang Z, Hou X, Lennartsson J, Li Y, Koch AW, Scotney P, Lee C, Arjunan P, Dong L, et al. VEGF-B is dispensable for blood vessel growth but critical for their survival, and VEGF-B targeting inhibits pathological angiogenesis. *Proc Natl Acad Sci USA*. 2009;106:6152–6157. doi: 10.1073/pnas.0813061106
45. Pinto AR, Ilinykh A, Ivey MJ, Kuwabara JT, D'Antoni ML, Debuque R, Chandran A, Wang L, Arora K, Rosenthal NA, et al. Revisiting cardiac cellular composition. *Circ Res*. 2016;118:400–409. doi: 10.1161/CIRCRESAHA.115.307778
46. Van Lint J, Rykx A, Maeda Y, Vantus T, Sturany S, Malhotra V, Vandenheede JR, Seufferlein T. Protein kinase D: an intracellular traffic regulator on the move. *Trends Cell Biol*. 2002;12:193–200. doi: 10.1016/s0962-8924(02)02262-6
47. Shafat I, Vlodavsky I, Ilan N. Characterization of mechanisms involved in secretion of active heparanase. *J Biol Chem*. 2006;281:23804–23811. doi: 10.1074/jbc.M602762200
48. Nadav L, Eldor A, Yacoby-Zeevi O, Zamir E, Pecker I, Ilan N, Geiger B, Vlodavsky I, Katz BZ. Activation, processing and trafficking of extracellular heparanase by primary human fibroblasts. *J Cell Sci*. 2002;115:2179–2187. doi: 10.1242/jcs.115.10.2179
49. Vidak E, Javorsek U, Vizovisek M, Turk B. Cysteine cathepsins and their extracellular roles: shaping the microenvironment. *Cells*. 2019;8:8. doi: 10.3390/cells8030264
50. Huotari J, Helenius A. Endosome maturation. *EMBO J*. 2011;30:3481–3500. doi: 10.1038/emboj.2011.286
51. Vlodavsky I, Ilan N, Naggi A, Casu B. Heparanase: structure, biological functions, and inhibition by heparin-derived mimetics of heparan sulfate. *Curr Pharm Des*. 2007;13:2057–2073. doi: 10.2174/138161207781039742
52. Levy-Adam F, Miao HQ, Heinrikson RL, Vlodavsky I, Ilan N. Heterodimer formation is essential for heparanase enzymatic activity. *Biochem Biophys Res Commun*. 2003;308:885–891. doi: 10.1016/s0006-291x(03)01478-5
53. Takenouchi T, Nakai M, Iwamaru Y, Sugama S, Tsukimoto M, Fujita M, Wei J, Sekigawa A, Sato M, Kojima S, et al. The activation of P2X7 receptor impairs lysosomal functions and stimulates the release of autophagolysosomes in microglial cells. *J Immunol*. 2009;182:2051–2062. doi: 10.4049/jimmunol.0802577
54. Bellin RM, Kubicek JD, Frigault MJ, Kamien AJ, Steward RL Jr, Barnes HM, Digiacomo MB, Duncan LJ, Edgerly CK, Morse EM, et al. Defining the role of syndecan-4 in mechanotransduction using surface-modification approaches. *Proc Natl Acad Sci USA*. 2009;106:22102–22107. doi: 10.1073/pnas.0902639106
55. Buchanan C, Stigliano I, Garay-Malpartida HM, Rodrigues Gomes L, Puricelli L, Sogayar MC, de Kier B, Joffe E, Peters MG. Glypican-3 re-expression regulates apoptosis in murine adenocarcinoma mammary cells modulating PI3K/Akt and p38MAPK signaling pathways. *Breast Cancer Res Treat*. 2010;119:559–574. doi: 10.1007/s10549-009-0362-9
56. Kuriyama S, Mayor R. A role for Syndecan-4 in neural induction involving ERK- and PKC-dependent pathways. *Development*. 2009;136:575–584. doi: 10.1242/dev.027334
57. Yoneda A, Couchman JR. Regulation of cytoskeletal organization by syndecan transmembrane proteoglycans. *Matrix Biol*. 2003;22:25–33. doi: 10.1016/s0945-053x(03)00010-6
58. Moon JJ, Matsumoto M, Patel S, Lee L, Guan JL, Li S. Role of cell surface heparan sulfate proteoglycans in endothelial cell migration and mechanotransduction. *J Cell Physiol*. 2005;203:166–176. doi: 10.1002/jcp.20220
59. Pulinilkunnil T, Rodrigues B. Cardiac lipoprotein lipase: metabolic basis for diabetic heart disease. *Cardiovasc Res*. 2006;69:329–340. doi: 10.1016/j.cardiores.2005.09.017
60. van der Vusse GJ, van Bilsen M, Glatz JF. Cardiac fatty acid uptake and transport in health and disease. *Cardiovasc Res*. 2000;45:279–293. doi: 10.1016/s0008-6363(99)00263-1
61. Zechner R, Kienesberger PC, Haemmerle G, Zimmermann R, Lass A. Adipose triglyceride lipase and the lipolytic catabolism of cellular fat stores. *J Lipid Res*. 2009;50:3–21. doi: 10.1194/jlr.R800031-JLR200
62. Rodrigues B, Cam MC, Jian K, Lim F, Sambandam N, Shepherd G. Differential effects of streptozotocin-induced diabetes on cardiac lipoprotein lipase activity. *Diabetes*. 1997;46:1346–1353. doi: 10.2337/diab.46.8.1346
63. Kim MS, Wang F, Puthanveetil P, Kewalramani G, Innis S, Marzban L, Steinberg SF, Webber TD, Kieffer TJ, Abrahani A, et al. Cleavage of protein kinase D after acute hypoinsulinemia prevents excessive lipoprotein lipase-mediated cardiac triglyceride accumulation. *Diabetes*. 2009;58:2464–2475. doi: 10.2337/db09-0681
64. Wang Y, Chiu AP, Neumaier K, Wang F, Zhang D, Hussein B, Lal N, Wan A, Liu G, Vlodavsky I, et al. Endothelial cell heparanase taken up by cardiomyocytes regulates lipoprotein lipase transfer to the coronary lumen after diabetes. *Diabetes*. 2014;63:2643–2655. doi: 10.2337/db13-1842
65. Zhu W, Guo S, Homilius M, Nsubuga C, Wright SH, Quan D, Kc A, Eddy SS, Victorio RA, Beerens M, et al. PIEZO1 mediates a mechanothrombotic pathway in diabetes. *Sci Transl Med*. 2022;14:eabk1707. doi: 10.1126/scitranslmed.abk1707

SUPPLEMENTAL MATERIAL

Figure S1. Ponceau image of perfusates

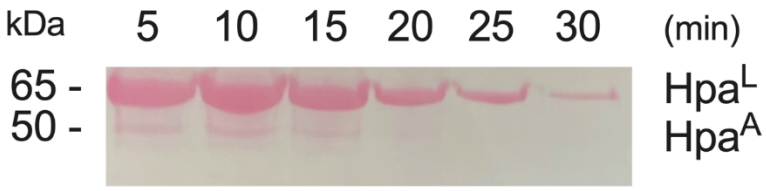

Following perfusion of isolated hearts for 30 min, the coronary effluent was collected and used for ponceau S staining for total protein normalization. The image corresponds to the Western blot described in Figure 1B. Hpa^A indicates active heparanase; Hpa^L, latent heparanase.

Figure S2. Heparanase gene expression in cardiac cells

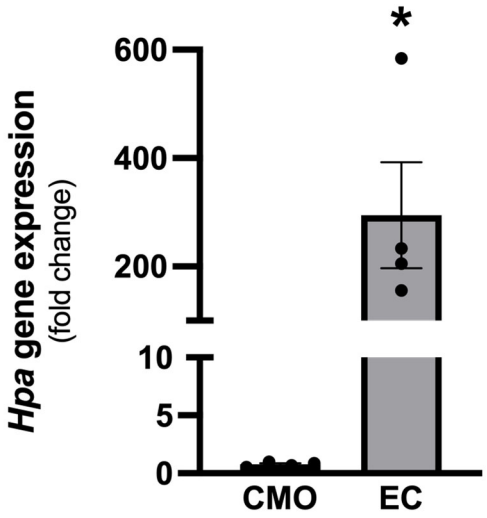

Cell lysates of primary rat cardiomyocytes (CMO) and EC were obtained for determination of heparanase gene expression. Data are presented as mean ± SEM; *Significantly different from CMO. *P<0.05 by the Student's t-test. CMO indicates cardiomyocytes; EC, endothelial cells; Hpa, heparanase.

Figure S3. Validation of laminar flow model

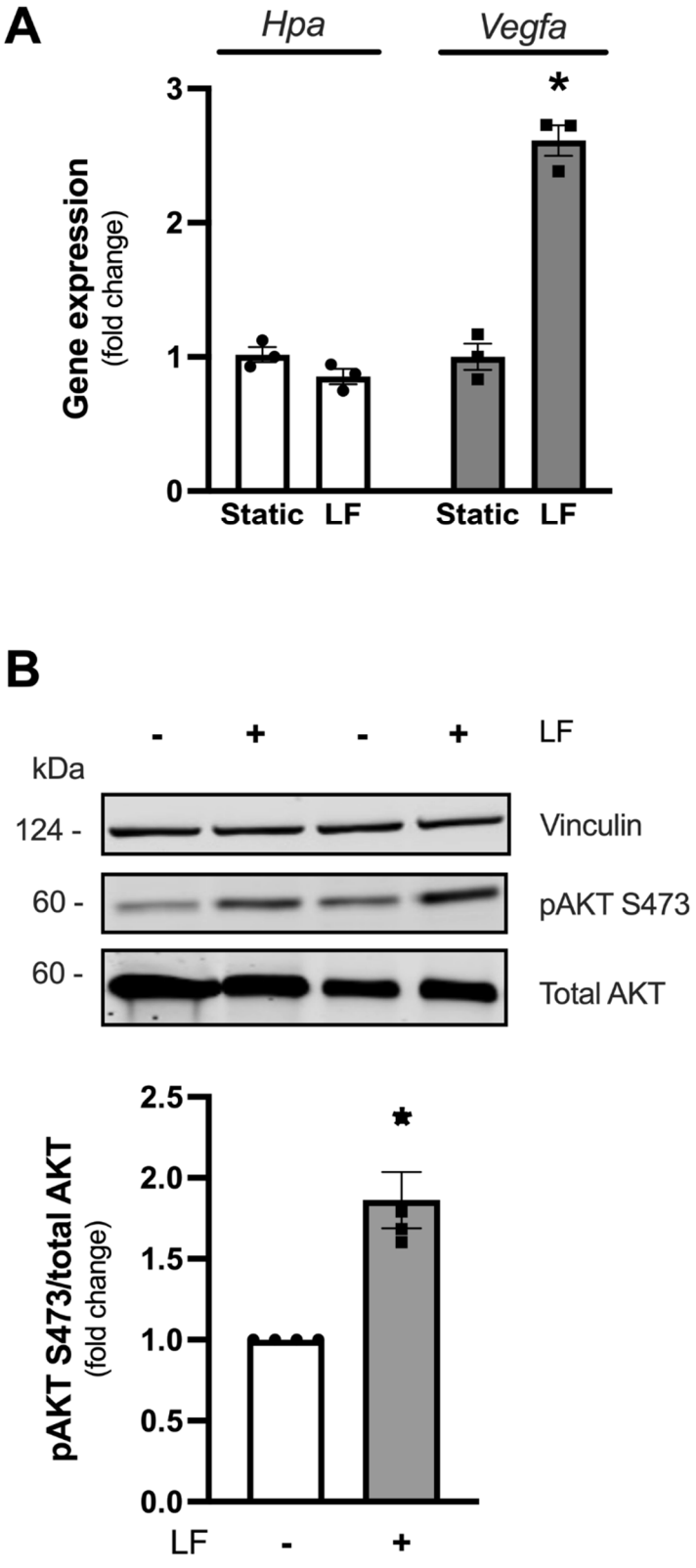

(A) EC were subjected to static or orbital shaking (LF) for 72 h, after which cell lysates were used for determination of heparanase and *Vegfa* gene expression. *Significantly different from static conditions. (B) EC were subjected to static or orbital shaking (LF) for 30 min, after which cell lysates were used for determination of AKT activation. *Significantly different from static conditions. All data are presented as mean ± SEM; *$P<0.05$ by the Student's *t*-test. EC indicates endothelial cells; Hpa, heparanase; LF, laminar flow; Vegfa, vascular endothelial growth factor A.

Figure S4. Piezo1 siRNA and response to laminar flow

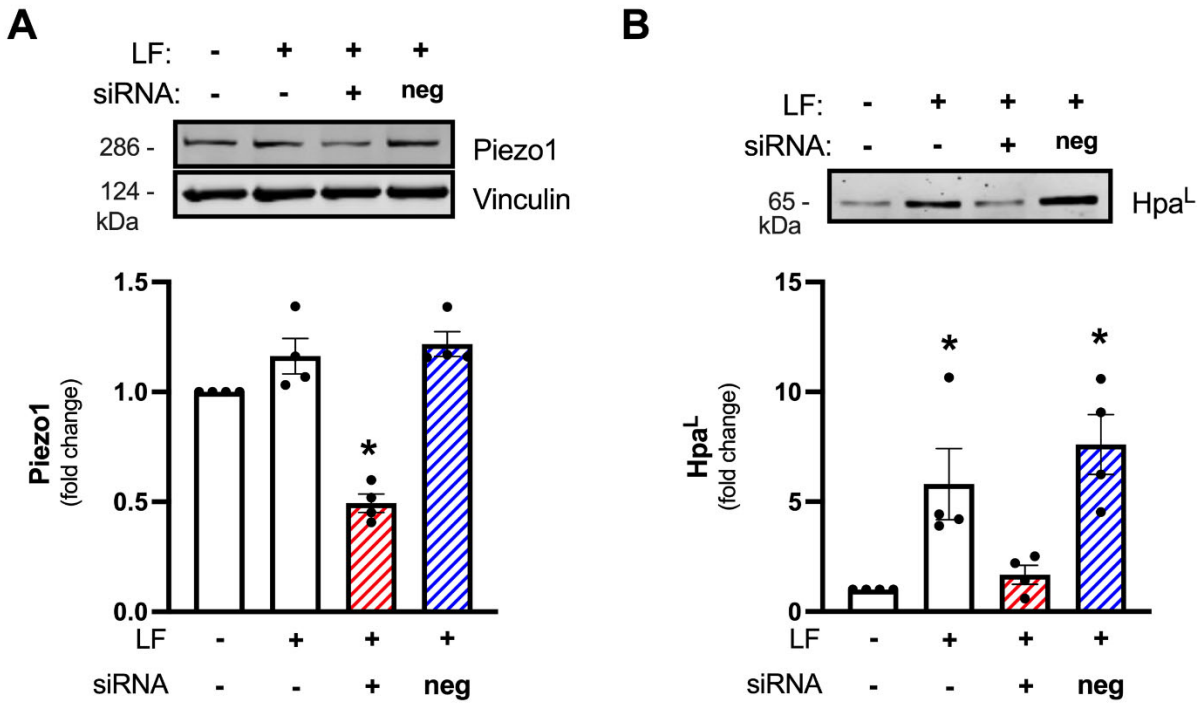

EC were transfected with Piezo1 siRNA or negative control (neg). After 48 h, cells were washed with PBS followed by 30 min exposure to either static or LF conditions. (A) Cell lysates were collected for determination of Piezo1 expression. *Significantly different from static conditions. (B) Conditioned medium from the transfected cells were collected, concentrated, and analyzed for Hpa^{L} secretion. *Significantly different from static conditions. All data are presented as mean ± SEM; *P<0.05 by one-way ANOVA with Bonferroni's *post hoc* test. EC indicates endothelial cells; Hpa^{L}, latent heparanase; LF, laminar flow; neg, siRNA negative control.

Figure S5. Piezo1-specific inhibition and response to laminar flow

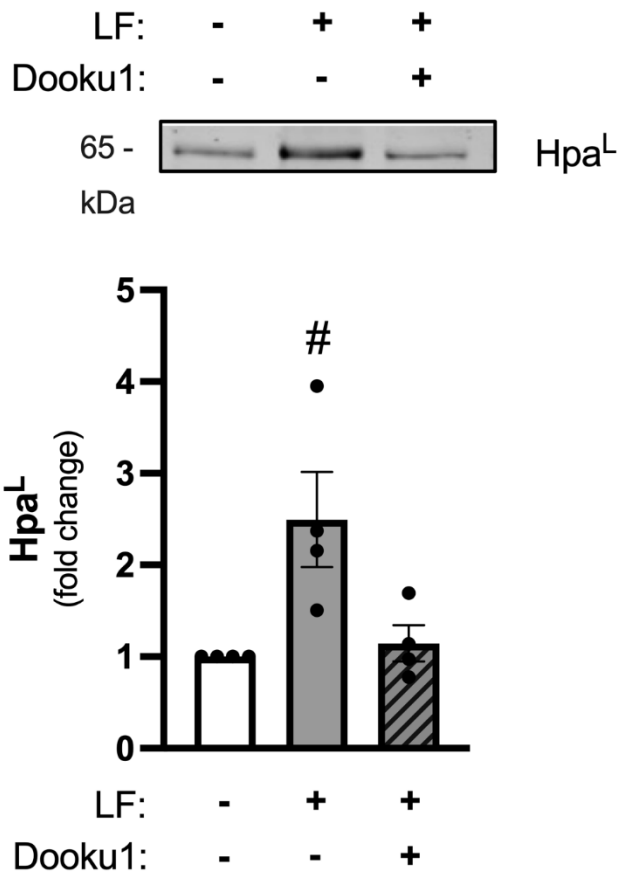

EC were pre-incubated with 10 μM of Dooku1, a selective antagonist of Piezo1. Subsequently cells were exposed to 30 min orbital rotation and latent heparanase determined in the incubation medium using Western blot. #Significantly different from all other groups. Data are presented as mean ± SEM; $P<0.05$ by one-way ANOVA with Bonferroni's *post hoc* test. EC indicates endothelial cells; Hpa^L, latent heparanase; LF, laminar flow.

Figure S6. Endothelial cells response to high glucose in releasing latent heparanase

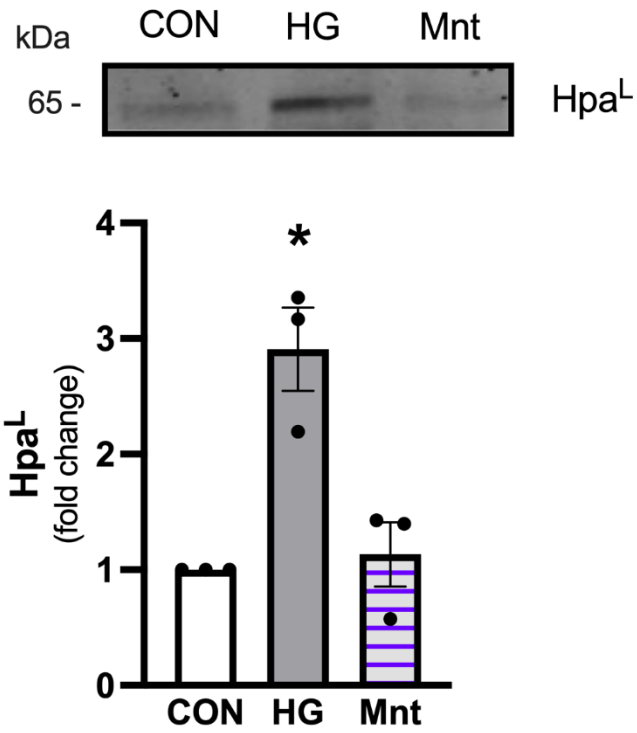

EC were exposed for 30 min to either 25 mM glucose (high glucose; HG) or the osmotic control, mannitol (Mnt). Conditioned medium was collected, concentrated, and analyzed for Hpa^{L}. Data are presented as mean ± SEM; *Significantly different from control (5.5 mM glucose) conditions. *P<0.05 by one-way ANOVA with Bonferroni's *post hoc* test. CON indicates control; EC, endothelial cells; HG, high glucose; Hpa^{L}, latent heparanase; Mnt, mannitol.

Figure S7. Piezo1-specific activation and EC response to release ATP and phosphorylate PKD

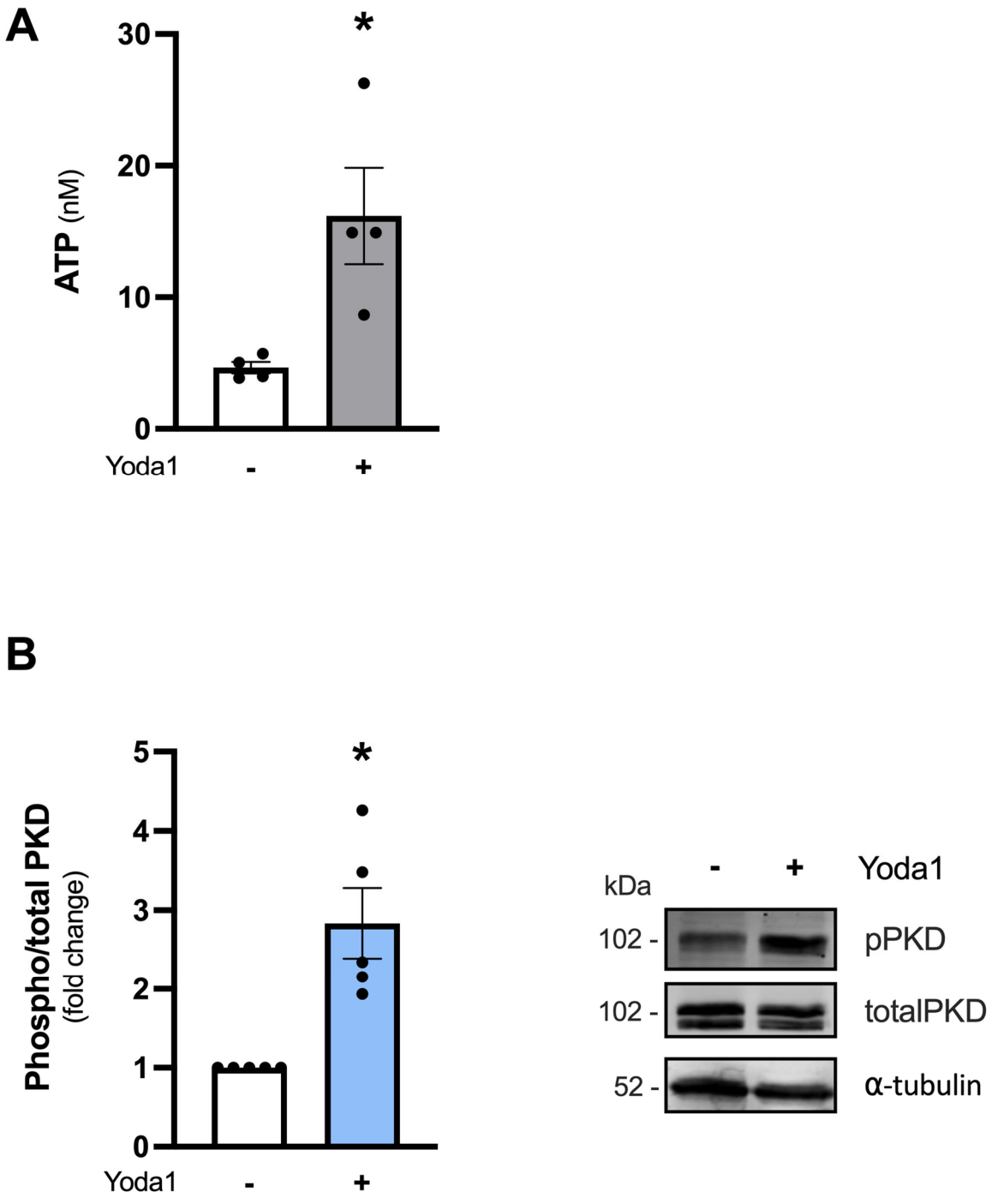

(A) Medium ATP secretion was measured using medium samples from EC exposed to Yoda1 (10 μM). *Significantly different from the control condition. (B) EC were treated with Yoda1 for 30 min, and the lysates analyzed for phosphorylation of PKD. *Significantly different from

control. All data are presented as mean ± SEM: *P<0.05 by the Student's t-test. EC indicates endothelial cells; PKD, protein kinase D.

Figure S8. Thrombin activation of cardiomyocytes and its intracellular signaling

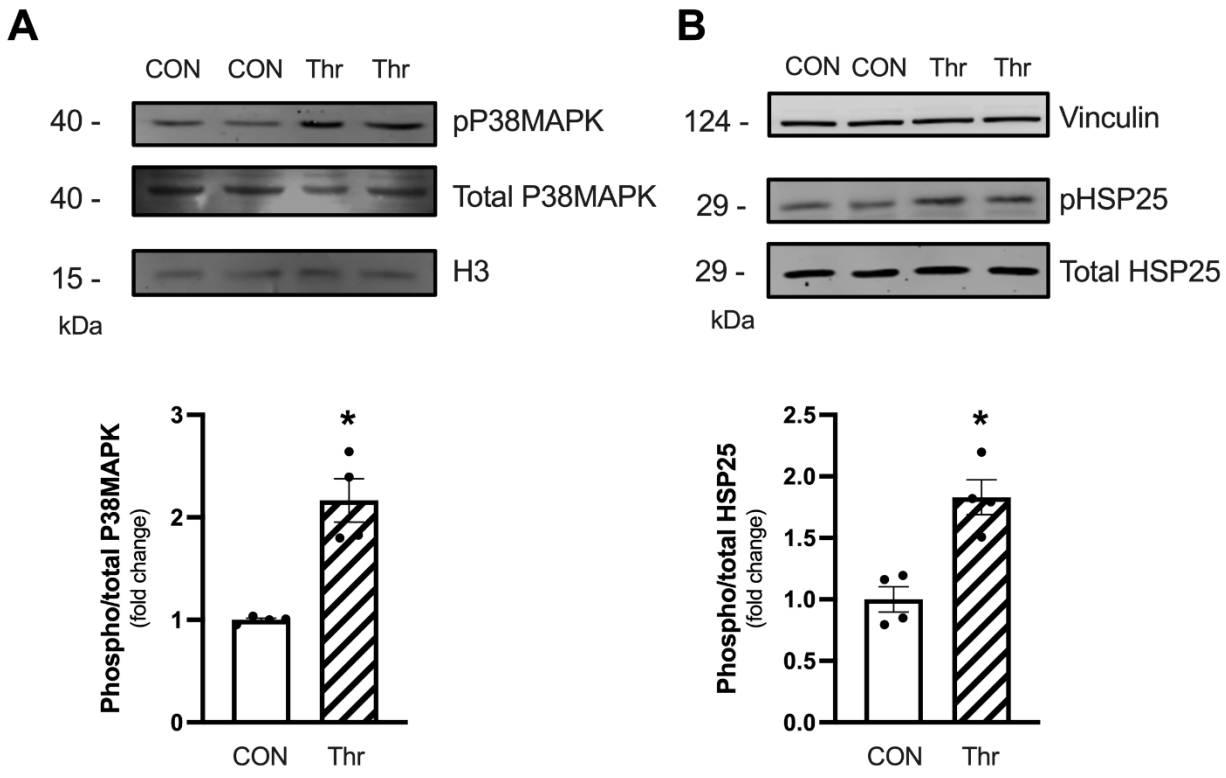

Cardiomyocytes were incubated with thrombin (0.05 U/mL) for 1 h and examined for (A) nuclear phosphorylation of p38MAPK and (B) cytoplasmic phosphorylation of HSP25. *Significantly different from control. All data are presented as mean ± SEM; *P<0.05 by the Student's t-test. CON indicates control; H3, nuclear loading control histone; Thr, thrombin.

Figure S9. Time-course treatment of EC with HG and determination of Piezo1 expression

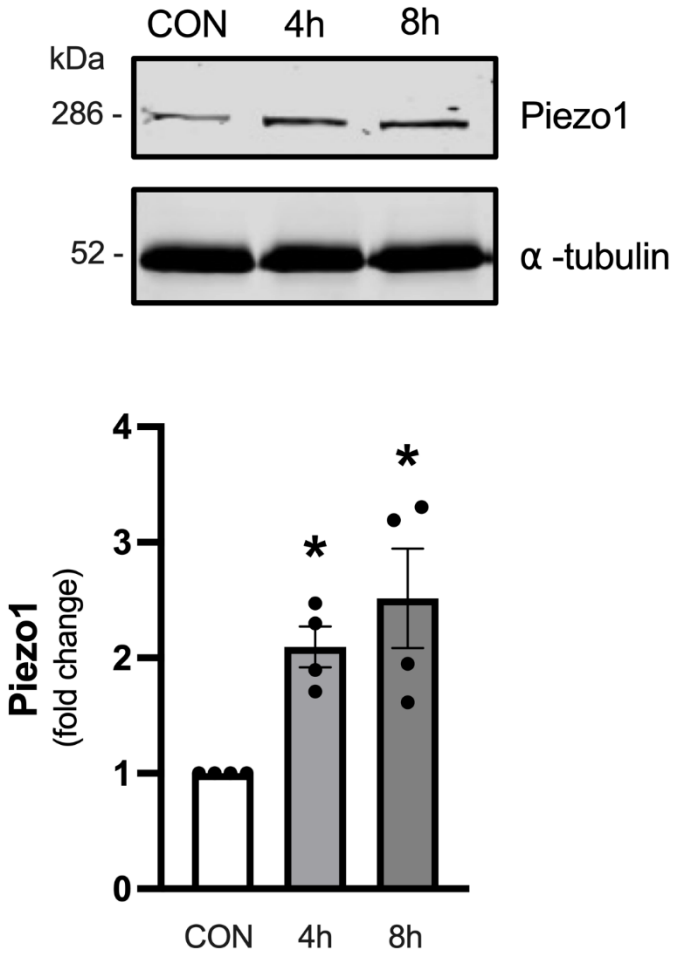

EC were exposed for 4 and 8 h to 25 mM glucose. Cell lysates were collected for determination of Piezo1. Data are presented as mean ± SEM; *Significantly different from control (5.5 mM glucose) conditions. *P<0.05 by one-way ANOVA with Bonferroni's *post hoc* test. CON indicates control; EC, endothelial cells.

Figure S10. Piezo1 expression in EC following high glucose and mannitol

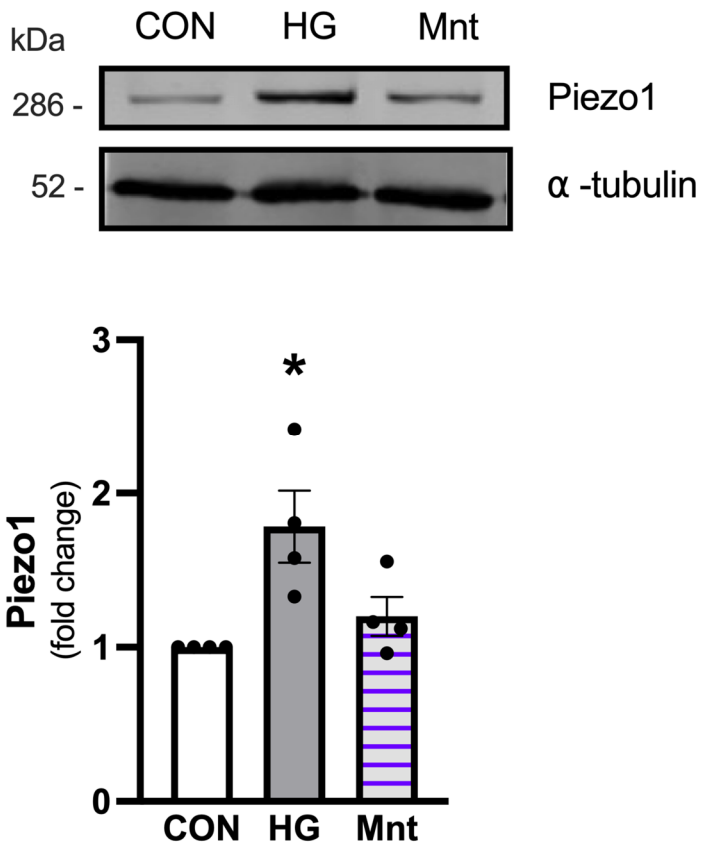

EC were exposed for 24 h to either 25 mM glucose (high glucose; HG) or the osmotic control, mannitol (Mnt). Cell lysates were collected for determination of Piezo1. Data are presented as mean ± SEM; *Significantly different from control (5.5 mM glucose) conditions. *P<0.05 by one-way ANOVA with Bonferroni's *post hoc* test. CON indicates control; EC, endothelial cells; HG, high glucose; Mnt, mannitol.

Figure S11. Laminar flow mediates the crosstalk between endothelial cells and cardiomyocytes to regulate cardiac metabolism

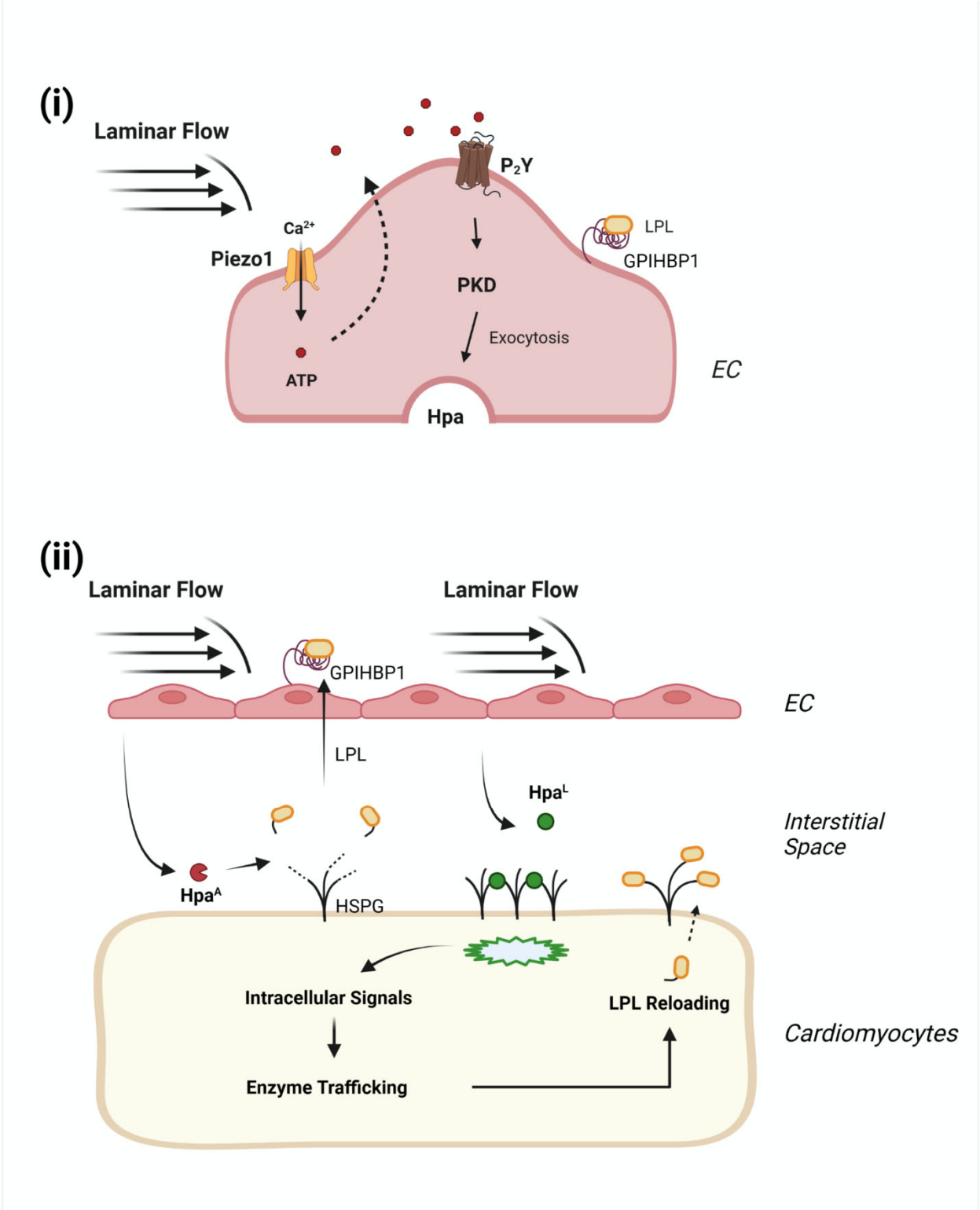

(i) Laminar flow activation of EC mechanosensors like Piezo1 causes downstream stimulation of purinergic receptors, PKD activation, and secretion of both Hpa^A and Hpa^L. (ii)

Cropping of heparan sulfate side chains on cardiomyocyte HSPG by Hpa^{A} releases cardiomyocyte LPL for its onward journey to the vascular lumen. The resulting heparan sulfate ends are permissive for clustering by Hpa^{L}, promoting downstream signaling which is critical for enzyme trafficking and LPL reloading onto cardiomyocyte HSPG. EC indicates endothelial cells; GPIHBP1, GPI-anchored high-density lipoprotein-binding protein 1; Hpa^{A}, active heparanase; Hpa^{L}, latent heparanase; HSPG, heparan sulfate proteoglycans; LPL, lipoprotein lipase; PKD, protein kinase D; P_2Y, purinergic receptor.